

Supporting Information

**Light-controlled cooperative catalysis of asymmetric
sulfoxidation based on azobenzene-bridged chiral
salen Ti^{IV} catalysts**

CONTENTS:

1. Synthetic details of azobenzene-bridged bimetallic chiral salenTi^{IV} catalysts (denoted as **ATGC-n**, n= 0, 2, 3, 4).
2. Identification of catalysts (**ATGC-n**, n= 0, 2, 3, 4) and the intermediates.
3. Evaluation of catalytic activity of **ATGC-n** in asymmetric sulfoxidation.

1. Synthetic details of azobenzene-bridged bimetallic chiral salen Ti^{IV} catalysts (denoted as ATGC-**n**, n= 0, 2, 3, 4)

1.1 Materials and reagents

4,4'-dihydroxyazobenzene, *tert*-butyl *N*-(2-bromoethyl)carbamate, *tert*-butyl *N*-(3-bromopropyl)carbamate and *tert*-butyl *N*-(4-bromopropyl)carbamate were purchased from Aldrich. The *tetra*-isopropyl titanate, phenyl methyl sulfide, phenyl ethyl sulfide, *p*-methoxyphenyl methyl sulfide, *o*-methoxyphenyl methyl sulfide, and *p*-bromophenyl methyl sulfide were obtained from J&K. 2-*tert*-Butyl phenol was purchased from Alfa Aesar. Other commercially available chemicals were laboratory grade reagents from local suppliers. (R,R)-*N*-(3,5-*di-tert*-butylsalicylidene)-*N*-(3-*tert*-butyl-5-chloro-methylsalicylidene)-1,2-cyclohexanediamine (denoted as CL) was synthesized as described procedure in corresponding reference.¹ [*N,N'*-Bis(3,5-*di-tert*-butyl salicylidene)-1,2-cyclohexanediaminato]titanium(IV) *di*-isopropyl (denoted as Neat-C, as shown in Chart S1) was prepared according to described procedures.² Phenyl *n*-butyl sulfide, and phenyl *n*-hexyl sulfide were synthesized according to Ref.³

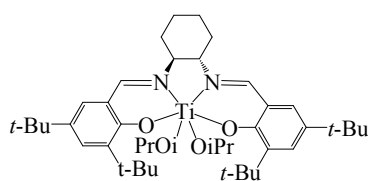


Chart S1 The structure of Neat-C.

1.2 Methods

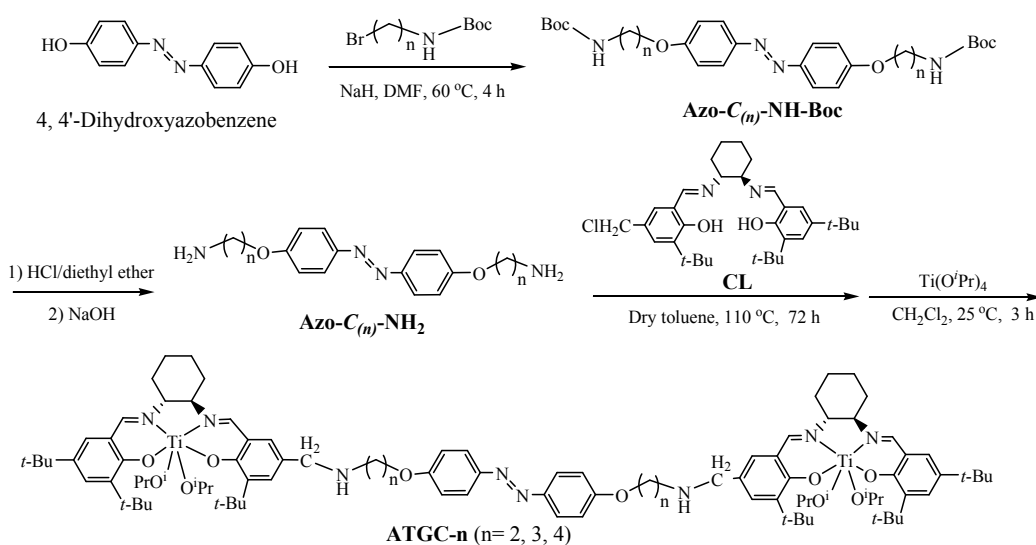
FT-IR spectra were obtained from potassium bromide pellets with a resolution of 4 cm⁻¹ and 64 scans in the range 400–4000 cm⁻¹ using an AVATAR 370 Thermo Nicolet spectrophotometer. UV-visible absorption spectra were measured on a UV/Vis Agilent 8453 spectrophotometer using a 10

mm path length quartz cell. The irradiation lamp was a UV lamp with $\lambda_{\text{max}} = 365$ nm. Samples were exposed to air during irradiation. NMR was recorded at a BRUKER AVANCE-500 spectrometer with TMS as an internal standard. All irradiations were performed directly in the Quartz NMR tubes. The measurements were repeated for at least three times to ensure good reproducibility. *Trans/cis* isomers ratios were obtained from the integrations of the signals from aromatic protons in corresponding isomers. Elemental analyses of C, H and N were carried out on Vario EL III Elemental analyses made in Germany. Contents of titanium in the samples were determined by inductively coupled plasma mass spectrometry (ICP-MS) on a NexION 300X analyzer (Perkin-Elmer Corp.). The optical rotation of samples was measured in dichloromethane on a WZZ-2A Automatic Polarimeter.

1.3 Preparation of azobenzene-bridged bimetallic chiral salenTi^{IV} catalysts (denoted as **ATGC-n**, where n represented the repeated methylene units in aliphatic linkers, n= 0, 2, 3, 4).

1.3.1 Preparation of **ATGC-n** (n= 2, 3, 4).

ATGC-n (n= 2, 3, 4) with various length of alkyl-terminated azobenzene spacers were prepared according to the procedure in Scheme S1.



Scheme S1 Synthesis of **ATGC-n** (n= 2, 3, 4)

Synthesis of Azo-C_(n)-NH-Boc (n= 2, 3, 4). 4, 4'-Dihydroxyazobenzene (0.96 g, 4.5 mmol) was dissolved in anhydrous DMF (30 mL). A suspension of sodium hydride (0.48 g, 12 mmol) in anhydrous DMF (10 mL) was slowly added into above solution. The mixture was stirred at room temperature until no bubble was observed. *N*-Benzyloxycarbonyl bromoalkylamines of Br(CH₂)_nNHBoc (10 mmol, n= 2, 3, 4) was then added into the stirring mixture. After being stirred at 60 °C for 4 h, the resulted mixture was poured into ice water (50 mL) and extracted with ether (3 × 10 mL). Combined organic phase was concentrated under vacuum. The crude product was further purified by crystallization from cold ethanol, giving **Azo-C_(n)-NH-Boc** (n= 2, 3, 4) as the yellow powders

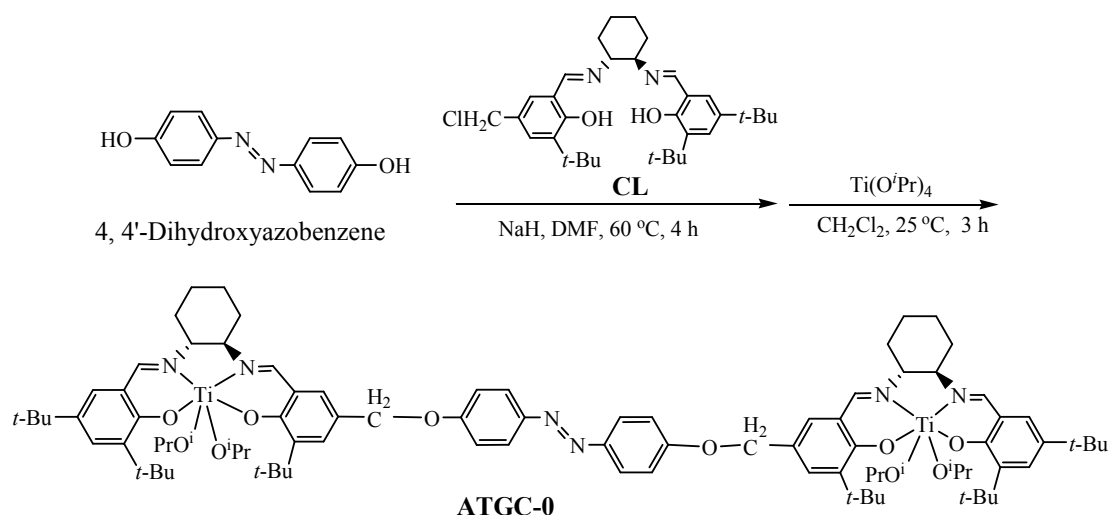
Synthesis of alkyl-terminated azobenzene linkers of Azo-C_(n)-NH₂ (n= 2, 3, 4). **Azo-C_(n)-NH-Boc** (n= 2, 3, 4) (3.0 mmol) was dissolved in a saturated solution of dry hydrogen bromide in ether (15 mL, 0.43 M) at 0 °C. The action mixture was stirred at 0 °C for 3 h, and then at 25 °C overnight. After removal of solvent, the resulting dark red solid was dissolved in water (50 mL). Aqueous sodium hydroxide (2.5 M) was used to adjust their pH value to 7.5. Crude product was extracted from the aqueous solutions with ether. Combined organic phase was washed with deionized water (3 × 15 mL), and concentrated under vacuum to afford **Azo-C_(n)-NH₂** (n= 2, 3, 4) as yellow powders

Synthesis of ATGC-n (n=2, 3, 4). The obtained **Azo-C_(n)-NH₂** (2.5 mmol) was mixed with asymmetric chiral salen ligand (CL, 3.23 g, 6.0 mmol) in dry toluene (15 mL) under room temperature. The mixture was refluxed for 72 h under argon and concentrated in vacuo. A residue was purified by column chromatography on silica gel using dichloromethane/methanol (4/1, v/v) as eluent. The resulting azobenzene-bridged chiral salen ligand was dissolved in dichloromethane, and followed by treatment with Ti(OⁱPr)₄ (1.76 g, 6.2 mmol) for 3 h at room temperature. After removal

of solvent, the crude product was washed with *n*-hexane (3 × 25 mL). The resulting orange solid was dissolved in dichloromethane (10 mL), and treated with water (2 mL) to remove any traces of TiO₂ by filtration. The filtrate was concentrated in vacuum and further dried in vacuum at 40 °C overnight, giving yellow powders of **ATGC-n** (n= 2, 3, 4).

1.3.2 Preparation of **ATGC-0**.

A control catalyst of **ATGC-0**, in which two Ti(salen) units was directly tethered with azobenzene, was prepared to evaluate the function of flexible alkyl spacer on cooperative catalysis. The preparation procedure was shown in Scheme S2. During the procedure, 4, 4'-dihydroxyazobenzene (0.54 g, 2.5 mmol) treated with sodium hydride (0.12 g, 5.1 mmol) was added into the CL (3.23 g, 6.0 mmol)-contained dimethyl formamide solution (30 mL). The mixture was stirred at 60 °C for 4 h under argon and concentrated in vacuo. The resulting azobenzene-bridged chiral salen ligand was dissolved in dichloromethane, and followed by treatment with Ti(O^{*i*}Pr)₄ (1.76 g, 6.2 mmol) for 3 h at room temperature. After removal of solvent, the crude product was washed with *n*-hexane (3 × 25 mL). The resulting orange solid was dissolved in dichloromethane (10 mL), and treated with water (2 mL) to remove any traces of TiO₂ by filtration. The filtrate was concentrated in vacuum and further dried in vacuum at 40 °C overnight, giving yellow powders of **ATGC-0**.

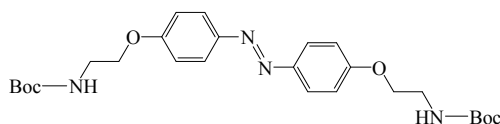


Scheme S2 Synthesis of **ATGC-0**.

2. Identification of the catalysts (**ATGC-n**, n=0, 2, 3, 4) and the intermediates.

2.1 Characterization of **Azo-C_(n)-NH-Boc** (n=2, 3, 4).

Azo-C₍₂₎-NH-Boc



Azo-C₍₂₎-NH-Boc (1.98 g, yield of 88%): Calc. for (C₂₆H₃₆N₄O₆): C: 62.38, H: 7.25, N: 11.19%.

Found: C: 62.37, H: 7.24, N: 11.21%. FT-IR (KBr): $\gamma_{\max}/\text{cm}^{-1}$ 3284, 2979, 2930, 1719, 1688, 1596, 1544, 1497, 1461, 1365, 1301, 1276, 1255, 1183, 1145, 1108, 1064, 842, 668. The structure of **Azo-C₍₂₎-NH-Boc** was further identified by ¹H NMR spectrum (see Figure S1). ¹H NMR (500 MHz, CDCl₃): δ (ppm): 7.85-7.83 (m, 4 H, ortho to -N=N- in azobenzene), 6.97-6.95 (m, 4 H, meta to -N=N- in azobenzene), 4.07 (m, 4 H, Ph-O-CH₂-), 3.54 (m, 4 H, -CH₂-NH-), 1.43 (m, 18 H, -OC(CH₃)₃ in Boc- group).

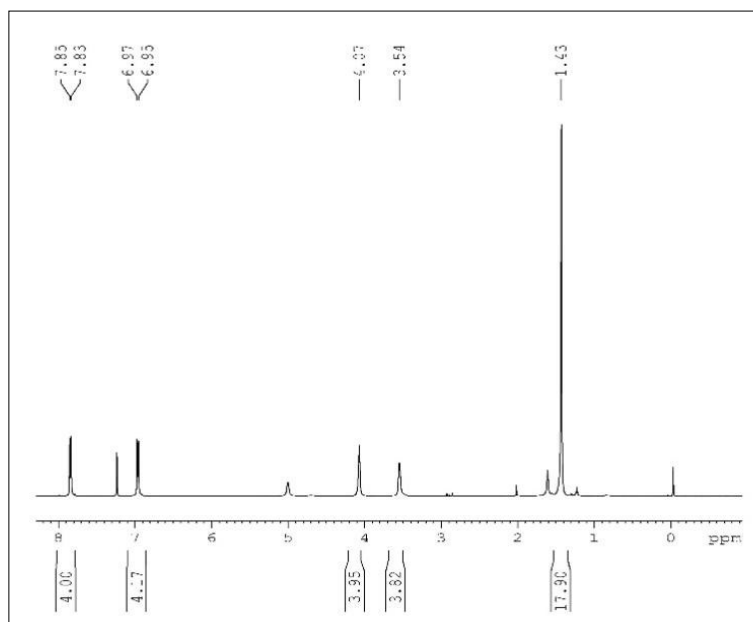
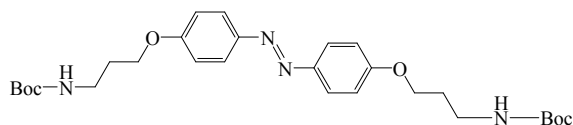


Figure S1 ^1H NMR of **Azo- $C_{(2)}$ -NH-Boc**.

Azo- $C_{(3)}$ -NH-Boc



Azo- $C_{(3)}$ -NH-Boc (1.99 g, yield of 84%): Calc. for $(\text{C}_{28}\text{H}_{40}\text{N}_4\text{O}_6)$: C: 63.62, H: 7.63, N: 10.6%.
 Found: C: 63.63, H: 7.61, N: 10.7%. FT-IR (KBr): $\gamma_{\text{max}}/\text{cm}^{-1}$ 3395, 2980, 2926, 1693, 1601, 1580, 1524, 1500, 1468, 1392, 1297, 1269, 1240, 1171, 1149, 1069, 938, 841, 668. The structure of **Azo- $C_{(3)}$ -NH-Boc** was further identified by ^1H NMR spectrum (see Figure S2). ^1H NMR (500 MHz, CDCl_3): δ (ppm): 7.84 (m, 4 H, ortho to $-\text{N}=\text{N}-$ in azobenzene), 6.96 (m, 4 H, meta to $-\text{N}=\text{N}-$ in azobenzene), 4.08 (m, 4 H, Ph-O-CH_2-), 3.33 (m, 4 H, $-\text{CH}_2-\text{CH}_2-\text{NH}-$), 2.00 (m, 4 H, $-\text{CH}_2-\text{CH}_2-\text{NH}-$), 1.43 (m, 18 H, $-\text{OC}(\text{CH}_3)_3$ in Boc- group).

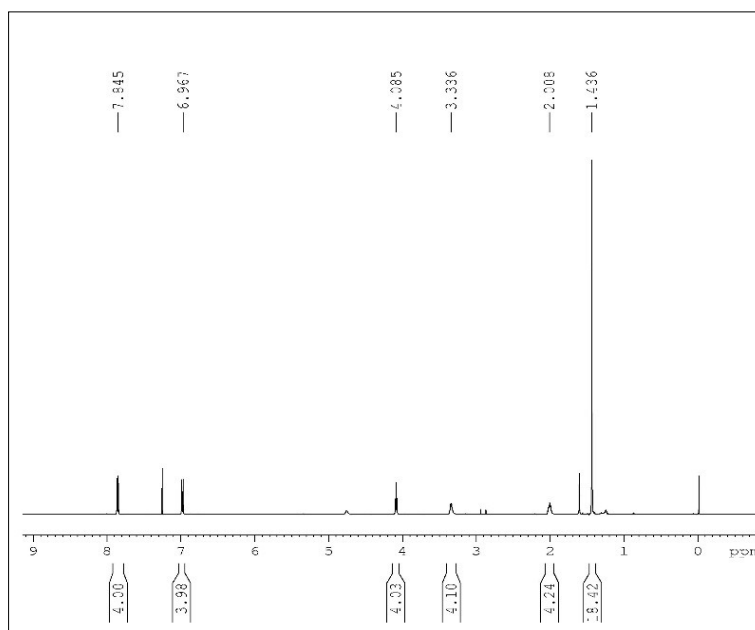
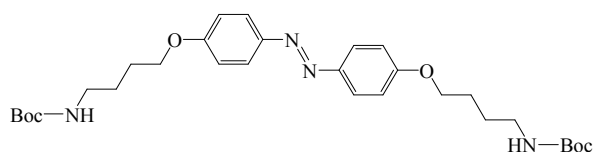


Figure S2 ^1H NMR of **Azo-C₍₃₎-NH-Boc**.

Azo-C₍₄₎-NH-Boc



Azo-C₍₄₎-NH-Boc (2.25 g, yield of 90%): Calc. for (C₃₀H₄₄N₄O₆): C: 64.73, H: 7.97, N: 10.06%.
 Found: C: 64.72, H: 7.98, N: 10.05%. FT-IR (KBr): $\gamma_{\text{max}}/\text{cm}^{-1}$ 3425, 2956, 2857, 1618, 1555, 1439, 1391, 1361, 1304, 1270, 1254, 1206, 1115, 1049, 846, 669. The structure of **Azo-C₍₄₎-NH-Boc** was further identified by ^1H NMR spectrum (see Figure S3). ^1H NMR (500 MHz, CDCl₃): δ (ppm): 7.84 (m, 4 H, ortho to -N=N- in azobenzene), 6.98 (m, 4 H, meta to -N=N- in azobenzene), 4.04 (m, 4 H, Ph-O-CH₂-), 3.20 (m, 4 H, -CH₂-CH₂-NH-), 1.84 (m, 4 H, Ph-OCH₂-CH₂-), 1.69 (m, 4 H, -CH₂-CH₂-NH-), 1.44 (m, 18 H, -OC(CH₃)₃ in Boc- group).

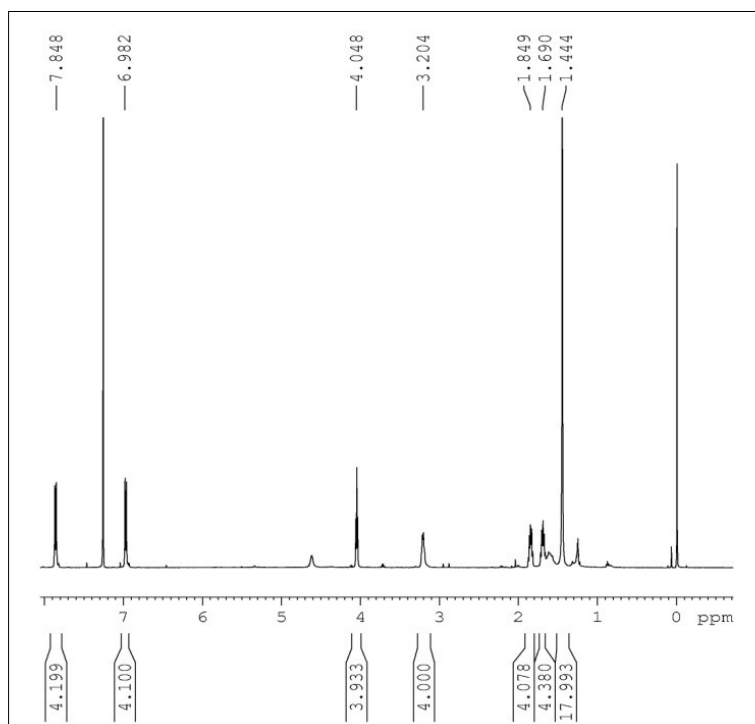
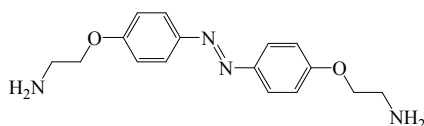


Figure S3 ^1H NMR of **Azo- $C_{(4)}$ -NH-Boc**.

2.2 Characterization of **Azo- $C_{(n)}$ -NH $_2$** (n= 2, 3, 4).

Azo- $C_{(2)}$ -NH $_2$



Azo- $C_{(2)}$ -NH $_2$ (0.82 g, yield of 91%): Calc. for ($\text{C}_{16}\text{H}_{20}\text{N}_4\text{O}_2$): C: 63.98, H: 6.71, N: 18.65%.

Found: C: 63.96, H: 6.72, N: 18.66%. FT-IR (KBr): $\gamma_{\text{max}}/\text{cm}^{-1}$ 3428, 3336, 2931, 1598, 1581, 1497,

1460, 1388, 1360, 1314, 1298, 1253, 1148, 1109, 1064, 843, 557. The structure of **Azo- $C_{(2)}$ -NH $_2$**

was further identified by ^1H NMR spectrum (see Figure S4). ^1H NMR (500 MHz, CDCl_3): δ (ppm):

7.87-7.85 (m, 4 H, ortho to -N=N- in azobenzene), 7.01-6.99 (m, 4 H, meta to -N=N- in azobenzene),

4.06 (m, 4 H, Ph-O- CH_2 -), 3.12 (m, 4 H, - CH_2 -NH $_2$).

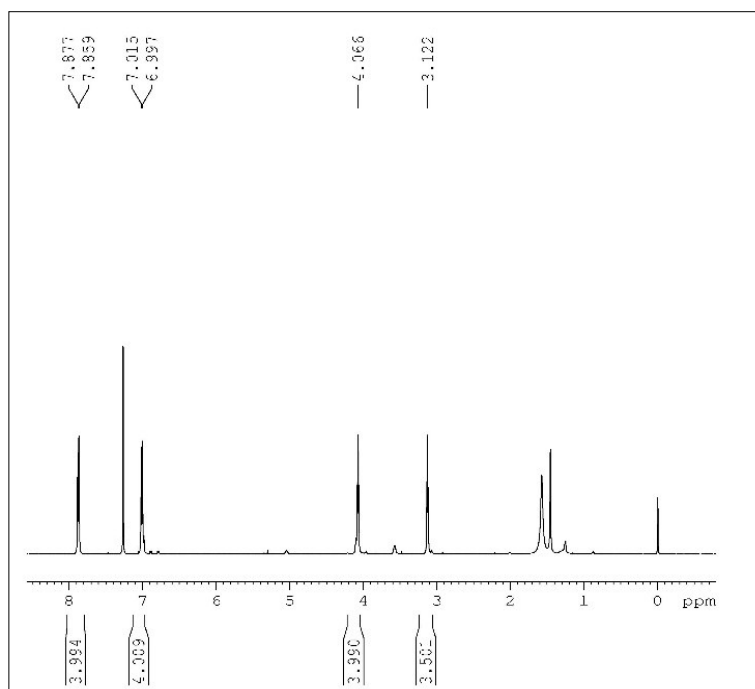
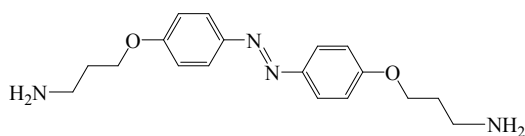


Figure S4 ^1H NMR of **Azo-C₍₂₎-NH₂**.

Azo-C₍₃₎-NH₂



Azo-C₍₃₎-NH₂ (0.92 g, yield of 93%): Calc. for (C₁₈H₂₄N₄O₂): C: 65.83, H: 7.37, N: 17.06%. Found: C: 65.82, H: 7.35, N: 17.08%. FT-IR (KBr): $\gamma_{\text{max}}/\text{cm}^{-1}$ 3449, 3339, 2929, 1601, 1598, 1495, 1470, 1387, 1357, 1311, 1296, 1242, 1151, 1108, 1055, 841, 556. The structure of **Azo-C₍₃₎-NH₂** was further identified by ^1H NMR spectrum (see Figure S5). ^1H NMR (500 MHz, DMSO-*d*₆): δ (ppm): 7.80 (m, 4 H, ortho to -N=N- in azobenzene), 7.10 (m, 4 H, meta to -N=N- in azobenzene), 4.12 (m, 4 H, Ph-O-CH₂-), 2.69 (m, 4 H, -CH₂-CH₂-NH₂), 1.80 (m, 4 H, -CH₂-CH₂-NH₂).

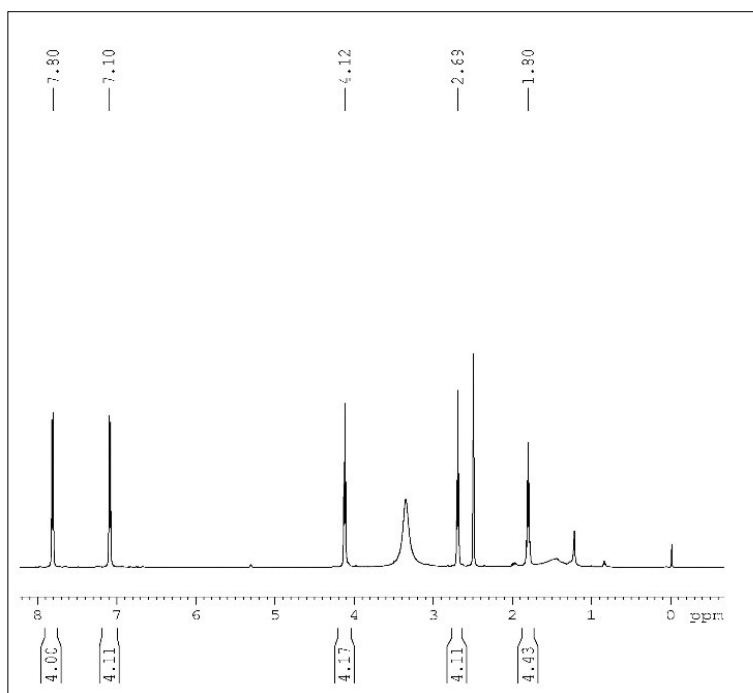
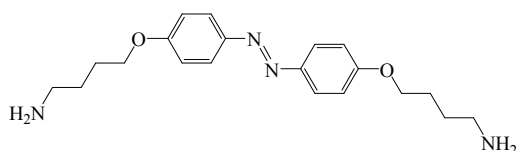


Figure S5 ^1H NMR of **Azo- $C_{(3)}$ - NH_2**

Azo- $C_{(4)}$ - NH_2



Azo- $C_{(4)}$ - NH_2 (1.0 g, yield of 94%): Calc. for $(\text{C}_{20}\text{H}_{28}\text{N}_4\text{O}_2)$: C: 67.39, H: 7.92, N: 15.72%.
 Found: C: 67.38, H: 7.93, N: 15.71%. FT-IR (KBr): $\gamma_{\text{max}}/\text{cm}^{-1}$ 3421, 3337, 2925, 1600, 1500, 1462, 1384, 1358, 1256, 1148, 1099, 1063, 948, 857, 543. The structure of **Azo- $C_{(4)}$ - NH_2** was further identified by ^1H NMR spectrum (see Figure S6). ^1H NMR (500 MHz, $\text{DMSO-}d_6$): δ (ppm): 7.84 (m, 4 H, ortho to -N=N- in azobenzene), 7.14 (m, 4 H, meta to -N=N- in azobenzene), 4.11 (m, 4 H, Ph-O- CH_2 -), 2.88 (m, 4 H, - CH_2 - CH_2 - CH_2 - NH_2), 1.83-1.76 (m, 8 H, - CH_2 - CH_2 - CH_2 - NH_2).

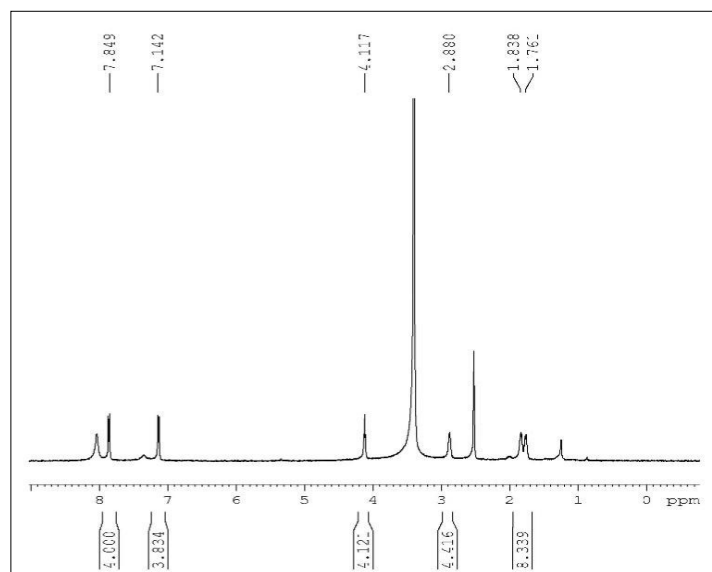
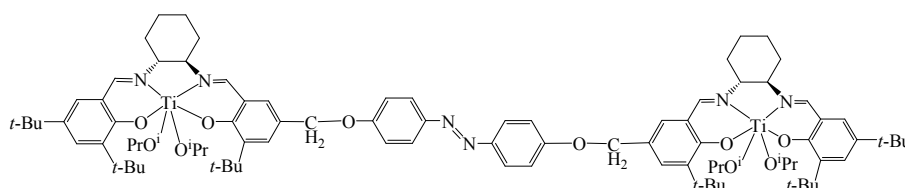


Figure S6 ^1H NMR of **Azo-C(4)-NH₂**.

2.3 Characterization of **ATGC-n** (n= 0, 2, 3, 4).

ATGC-0



ATGC-0 (2.23 g, yield of 68%): Calc. for (C₉₀H₁₂₆N₆O₁₀Ti₂): C: 69.84, H: 8.21, N: 5.43%.

Found: C: 69.86, H: 8.20, N: 5.42%. FT-IR (KBr): $\gamma_{\text{max}}/\text{cm}^{-1}$ 2948, 2868, 2676, 2603, 2494, 1612,

1543, 1487, 1439, 1392, 1362, 1270, 1172, 1028, 767, 709, 552. The structure of **ATGC-0** was

further identified by ^1H NMR (see Figure S7). ^1H NMR (500 MHz, CDCl₃): δ (ppm): 8.29 (m, 4 H,

Ph-HC=N-), 7.89 (m, 4 H, ortho to -N=N- in azobenzene), 7.59-7.04 (m, 8 H, Ph-H in Ti(salen)),

6.97 (m, 4 H, meta to -N=N- in azobenzene), 3.10-3.08 (m, 8 H, cyclohexyl-H and Ph-O-CH₂-

Ti(salen)), 2.29 (m, 4 H, CH₃-CH-CH₃ of ⁱPrO- in Ti(salen)), 1.44-1.41 (m, 16 H, cyclohexyl-H),

1.32-1.25 (m, 78 H, -CH₃ of *t*-Bu and ⁱPrO- in Ti(salen)). $\alpha_{25}^D = -20.1$ (c = 0.005 g. mL⁻¹, CH₂Cl₂),

titanium content: 0.31 mmol.g⁻¹.

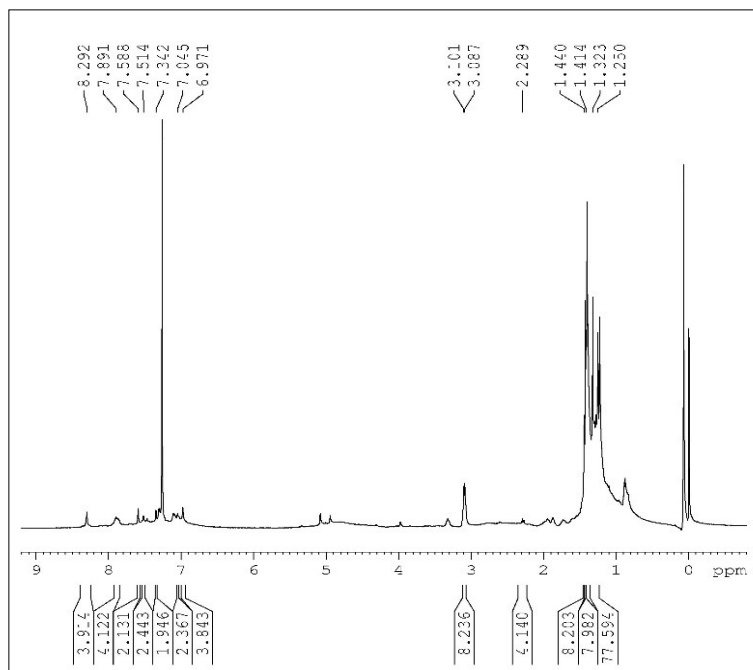
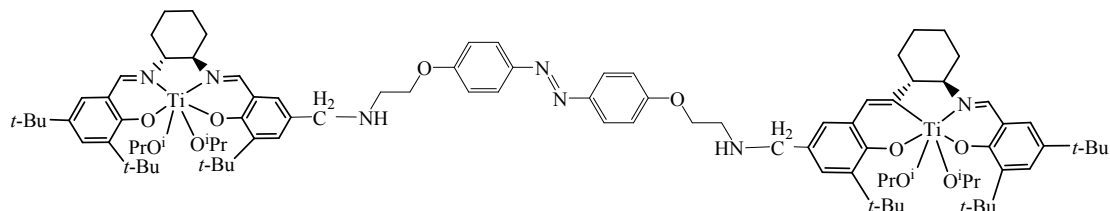


Figure S7 ^1H NMR of ATGC-0.

ATGC-2



ATGC-2 (2.65 g, yield of 76%): Calc. for ($\text{C}_{94}\text{H}_{136}\text{N}_8\text{O}_{10}\text{Ti}_2$): C: 69.10, H: 8.39, N: 6.86%.
 Found: C: 69.98, H: 8.40, N: 6.87%. FT-IR (KBr): $\gamma_{\text{max}}/\text{cm}^{-1}$ 3446, 2951, 2864, 1623, 1555, 1438, 1388, 1361, 1305, 1272, 1254, 1206, 1173, 1117, 1029, 865, 847, 773, 758, 682, 668, 590. The structure of **ATGC-2** was further identified by ^1H NMR (see Figure S8). ^1H NMR (500 MHz, CDCl_3): δ (ppm): 8.29 (m, 4 H, Ph- $\text{HC}=\text{N}$ -), 7.69 (m, 4 H, ortho to $-\text{N}=\text{N}$ - in azobenzene), 6.97-7.20 (m, 8 H, Ph- H in salen), 6.97 (m, 4 H, meta to $-\text{N}=\text{N}$ - in azobenzene), 4.32 (m, 4 H, Ph- $\text{O}-\text{CH}_2$ -), 3.46 (m, 4 H, $-\text{CH}_2-\text{CH}_2-\text{NH}$ -), 3.32-3.31 (m, 8 H, cyclohexyl- H and $-\text{NH}-\text{CH}_2-\text{Ti}(\text{salen})$),

2.22 (m, 4 H, CH₃-CH-CH₃ of ^{*i*}PrO- in Ti(salen)), 1.69-1.43 (m, 16 H, cyclohexyl-*H*), 1.35-1.28 (m, 78 H, -CH₃ of *t*-Bu and ^{*i*}PrO- in Ti(salen)). $\alpha_{25}^D = -19.3$ ($c = 0.005$ g. mL⁻¹, CH₂Cl₂), titanium content: 0.21 mmol. g⁻¹.

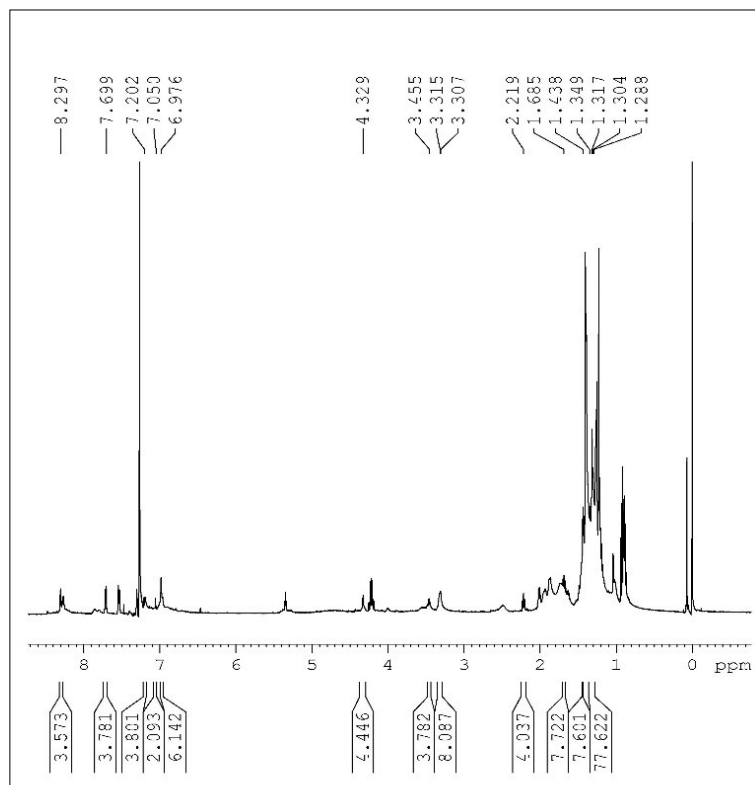
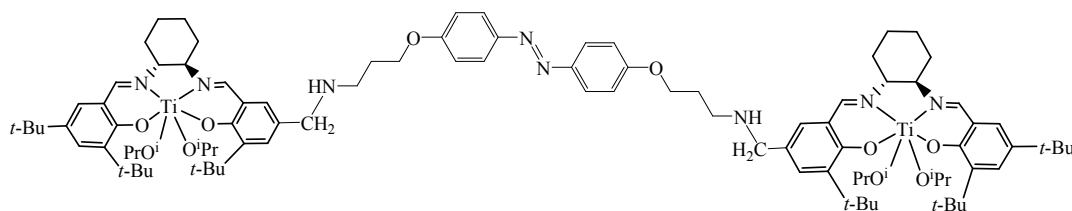


Figure S8 ¹H NMR of ATGC-2.

ATGC-3



ATGC-3 (2.6 g, yield of 73%): Calc. for (C₉₆H₁₄₀N₈O₁₀Ti₂): C: 69.38, H: 8.49, N: 6.74%. Found: C: 69.37, H: 8.51, N: 6.73%. FT-IR (KBr): $\gamma_{\max}/\text{cm}^{-1}$ 3424, 2956, 2862, 1615, 1555, 1438, 1463, 1391, 1361, 1303, 1271, 1254, 1206, 1175, 1116, 1072, 1027, 866, 847, 773, 758, 712, 670, 649, 584. The structure of **ATGC-3** was further identified by ¹H NMR (see Figure S9). ¹H NMR (500

MHz, CDCl₃): δ (ppm): 8.31 (m, 4 H, Ph-HC=N-), 7.86 (m, 4 H, ortho to -N=N- in azobenzene), 7.22-7.16 (m, 8 H, Ph-H in salen), 7.07 (m, 4 H, meta to -N=N- in azobenzene), 4.30 (m, 4 H, Ph-O-CH₂-), 3.59 (m, 4 H, -CH₂-CH₂-NH-), 3.37 (m, 8 H, cyclohexyl-H and -NH-CH₂-Ti(salen)), 2.71 (m, 4 H, -CH₂-CH₂-NH-), 2.23 (m, 4 H, CH₃-CH-CH₃ of ^{*i*}PrO- in Ti(salen)), 1.42-1.41 (m, 16 H, cyclohexyl-H), 1.33-1.29 (m, 78 H, -CH₃ of *t*-Bu and ^{*i*}PrO- in Ti(salen)). $\alpha_{25}^D = -21.5$ (c = 0.005 g. mL⁻¹, CH₂Cl₂), titanium content: 0.31 mmol. g⁻¹.

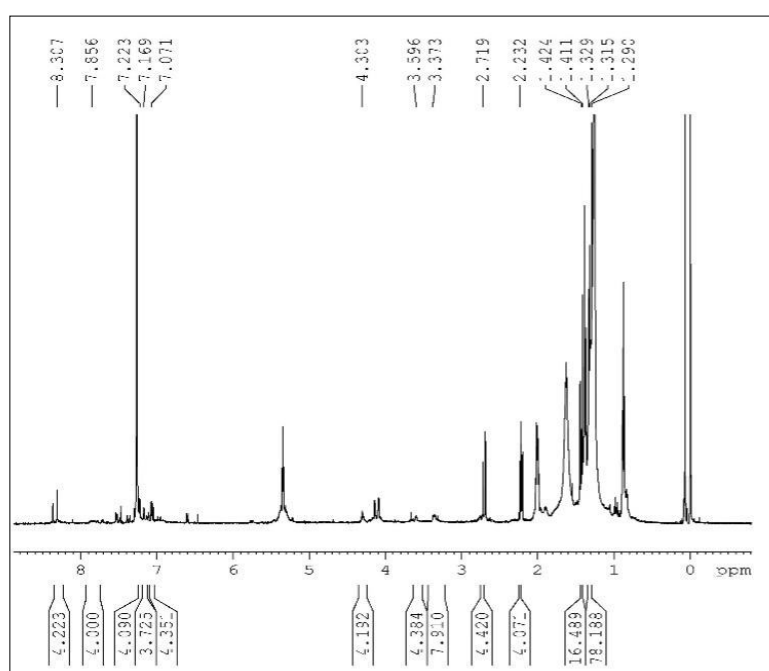
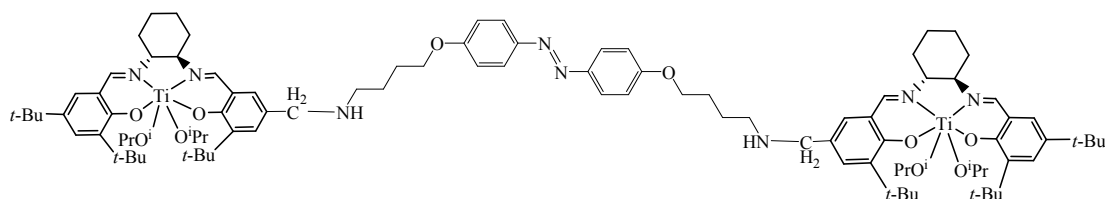


Figure S9 ¹H NMR of ATGC-3.

ATGC-4



ATGC-4 (2.80 g, yield of 77%). Calc. for (C₉₈H₁₄₄N₈O₁₀Ti₂): C: 69.65, H: 8.59, N: 6.63%.

Found: C: 69.63, H: 8.61, N: 6.64%. FT-IR (KBr): $\gamma_{\max}/\text{cm}^{-1}$ 3439, 2954, 2855, 1618, 1555, 1465,

1440, 1390, 1361, 1304, 1271, 1253, 1202, 1174, 1141, 1116, 866, 847, 773, 758, 696, 645, 582.

The structure of **ATGC-4** was further identified by ^1H NMR (see Figure S10). ^1H NMR (500 MHz, CDCl_3): δ (ppm): 8.41-8.34 (m, 4 H, Ph- $\text{HC}=\text{N}$ -), 7.88 (m, 4 H, ortho to $-\text{N}=\text{N}$ - in azobenzene), 7.25-7.08 (m, 8 H, Ph- H in salen), 7.01 (m, 4 H, meta to $-\text{N}=\text{N}$ - in azobenzene), 4.12 (m, 4 H Ph- $\text{O}-\text{CH}_2$ -), 3.38 (m, 8 H, cyclohexyl- H and $-\text{NH}-\text{CH}_2-\text{Ti}(\text{salen})$), 3.24 (m, 4 H, $-\text{CH}_2-\text{CH}_2-\text{NH}$ -), 2.78-2.72 (m, 8 H, $-\text{CH}_2-\text{CH}_2-\text{CH}_2-\text{NH}$ -), 2.24 (m, 4 H, $\text{CH}_3-\text{CH}-\text{CH}_3$ of ^iPrO - in $\text{Ti}(\text{salen})$), 1.46 (m, 16 H, cyclohexyl- H), 1.31-1.28 (m, 78 H, $-\text{CH}_3$ of t -Bu and ^iPrO - in $\text{Ti}(\text{salen})$). $\alpha_{25}^D = -24.2$ ($c = 0.005$ g. mL^{-1} , CH_2Cl_2), titanium content: 0.15 mmol. g^{-1} .

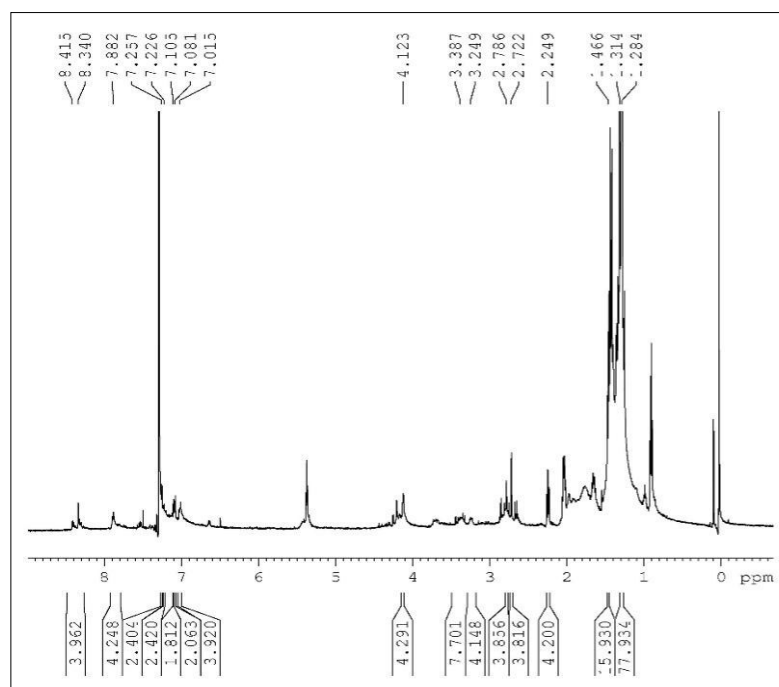


Figure S10 ^1H NMR of **ATGC-4**.

2.4 FT-IR

Successful bridging $\text{Ti}(\text{salen})$ units with $\text{Azo-}C_{(n)}-\text{NH}_2$ was confirmed by FT-IR spectroscopy.

ATGC-3 with a middling length of the aliphatic chain was chosen as the typical catalyst for the structural identification. Figure S11 showed the FT-IR spectra of **ATGC-3**, $\text{Azo-}C_{(3)}-\text{NH}_2$, as well

as Neat-C for comparison. Clearly, Azo- $C_{(3)}$ -NH₂ showed characteristic N-H stretching of terminal primary amino (-NH₂) group (3449 and 3339 cm⁻¹), N=N stretching of azobenzene (1598 cm⁻¹),⁴ and C-O-C stretching of the aromatic ether group (1242 and 1108 cm⁻¹) in its FT-IR spectrum (Fig. S11-a). After Ti(salen) modification, the bands corresponding to the primary amino (-NH₂) group disappeared with the formation of a new band at around 3435 cm⁻¹, which was the characteristic stretching vibration of N-H in the second amine (-NH-) group (Figure S11-c vs. S11-a). It provided convincing proof that the terminated amino group underwent N-alkylation with chloromethyl (-CH₂Cl) groups of the asymmetric salen ligand during the modification. Ti(salen) units were thus bridged with the Azo- $C_{(3)}$ -NH₂ linker, giving the azobenzene-bridged bimetallic Ti(salen) catalysts of ATGC-3. The successful linkage was also evident from the fact that ATGC-3 gave the characteristic bands assigned to the vibrations of C=N (1621 cm⁻¹), C-O (1547 cm⁻¹) and Ti-O (807 cm⁻¹) in Ti(salen) complex (Figure S11-c vs. S11-b). The characteristic bands were similar with that in Neat-C, suggesting the intact active site during the linkage.

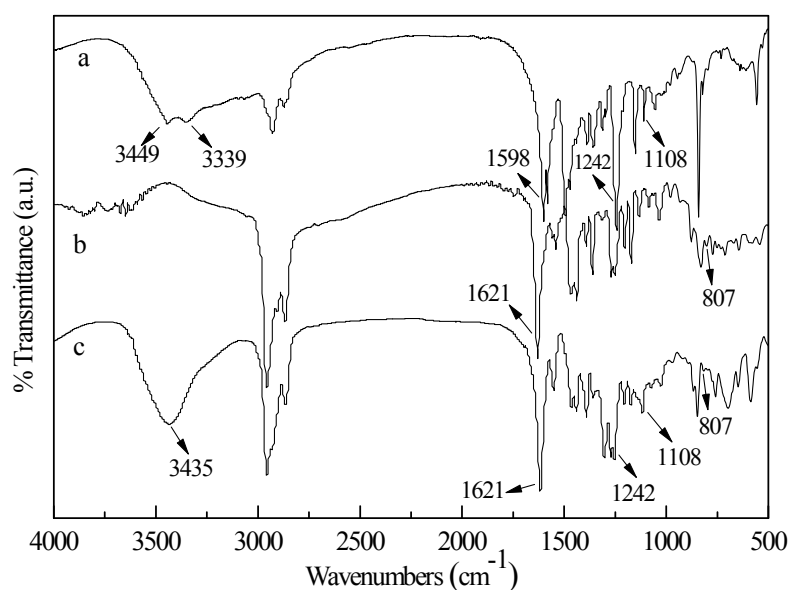


Figure S11 FT-IR spectra of Azo- $C_{(3)}$ -NH₂ (a), Neat-C (b) and ATGC-3 (c).

3. Evaluation of catalytic activity of **ATGC-n** in asymmetric sulfoxidation.

3.1 Catalytic performance

Before reaction, dark-adapted catalyst was exposed to UV light ($\lambda = 365$ nm) for 20 min to ensure the *cis*-state of azobenzene linker. The UV-treated catalyst (0.1 mol% of substrate, based on the titanium content in catalyst) was mixed with aryl alkyl sulfides (1.0 mmol) in ethanol (2 mL) under stirring at 25 °C. Aqueous hydrogen peroxide (*aq.* H₂O₂, 30 wt%, 1.2 mmol) was then dropwise added into the solution within 15 min. The resulting mixture was exposed to UV light and stirred at room temperature, until the reaction was judged to be complete based on GC analysis. And then, reaction mixture was extracted with ethyl acetate for five times (5×3 mL). The upper extracted solution was combined and concentrated in vacuo. Further purification of the residue by chromatography on silica gel (petroleum ether/ethyl acetate, 1.5/1) afforded pure chiral sulfoxides. The products have been identified by ¹H NMR spectra. Conversion and chemoselectivity to the chiral sulfoxides were measured by a 6890N gas chromatograph (Agilent Co.) equipped with a capillary column (HP19091G-B213, 30 m×0.32 mm×0.25 mm) and a FID detector. Enantiomer excess (ee) values of chiral products were determined by HPLC analysis using the Daicel Chiralpak AD columns.

Phenyl methyl sulfoxide: The product has been identified by ¹H NMR spectrum (see Figure S12). ¹H NMR (CDCl₃, 500 MHz): δ (ppm): 7.63-7.51 (m, 5 H, ArH), 2.72 (s, 3 H, -SCH₃). Chemoselectivity was determined by GC, nitrogen was used as the carrier gas with a flow of 30 mL.min⁻¹, injector temperature and detector temperature were 250 °C, column temperature was 150 °C, $t_{\text{Phenyl methyl sulfoxide}} = 5.5$ min. Ee value was determined by HPLC (*t*PrOH/ *n*-hexane = 1: 9 (v/v));

flow rate = 1.0 mL.min⁻¹; 25 °C; λ = 254 nm; major enantiomer t_R = 5.5 min, minor enantiomer t_S = 6.4 min (see Figure S13-S21). $[\alpha]_D = +115.3$ (c = 0.4 in acetone). lit: $[\alpha]_D = -130.1$ (c=1.7 in acetone) for (*S*), 90% ee.⁵

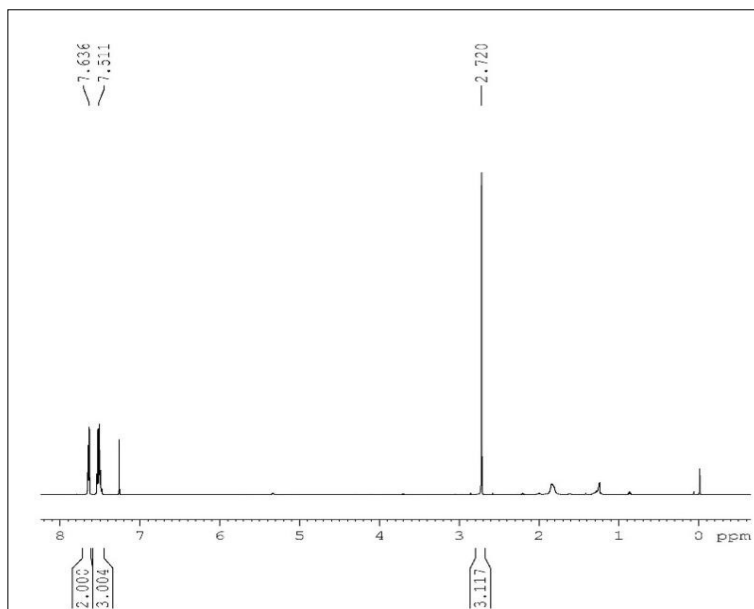


Figure S12 ¹H NMR of phenyl methyl sulfoxide.

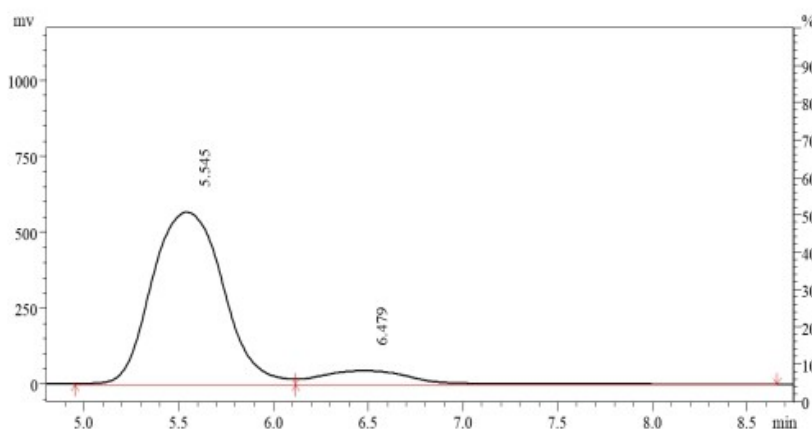


Figure S13 HPLC of phenyl methyl sulfoxide obtained over ATGC-0 under UV irradiation (ee value = 80%).

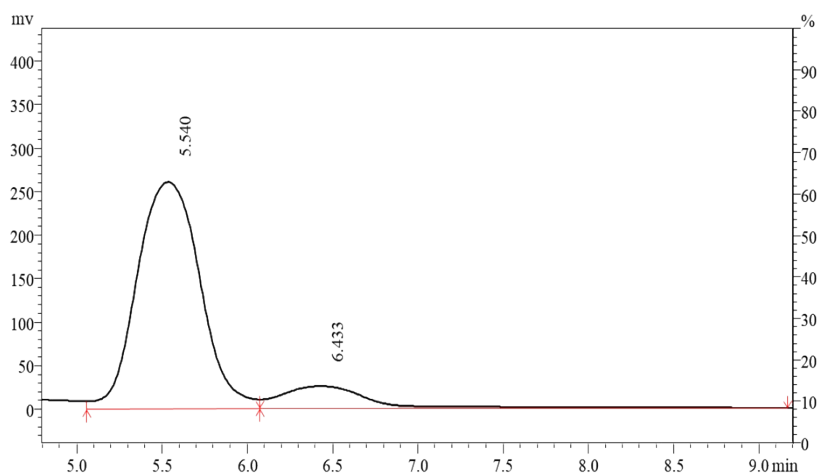


Figure S14 HPLC of phenyl methyl sulfoxide obtained over **ATGC-0** in dark (ee value = 75%).

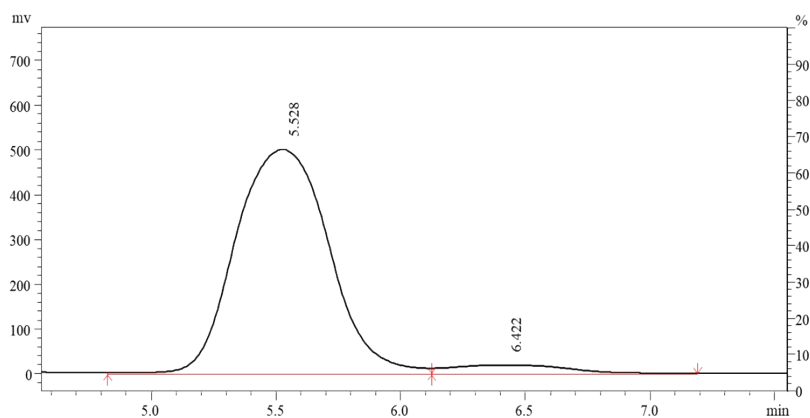


Figure S15 HPLC of phenyl methyl sulfoxide obtained over **ATGC-2** under UV irradiation (ee value = 90%).

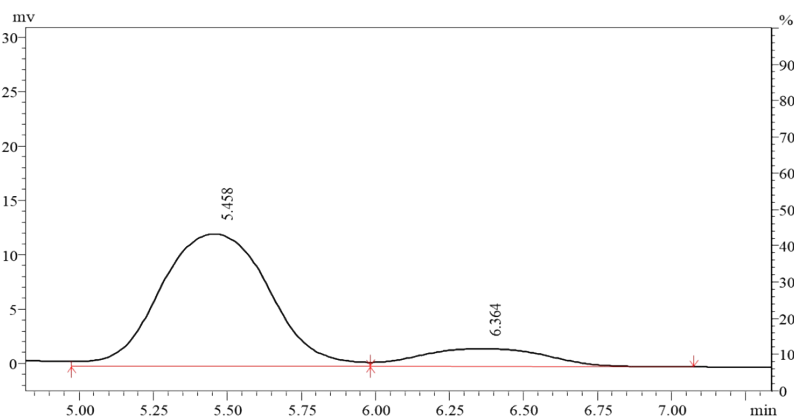


Figure S16 HPLC of phenyl methyl sulfoxide obtained over **ATGC-2** in dark (ee value = 75%).

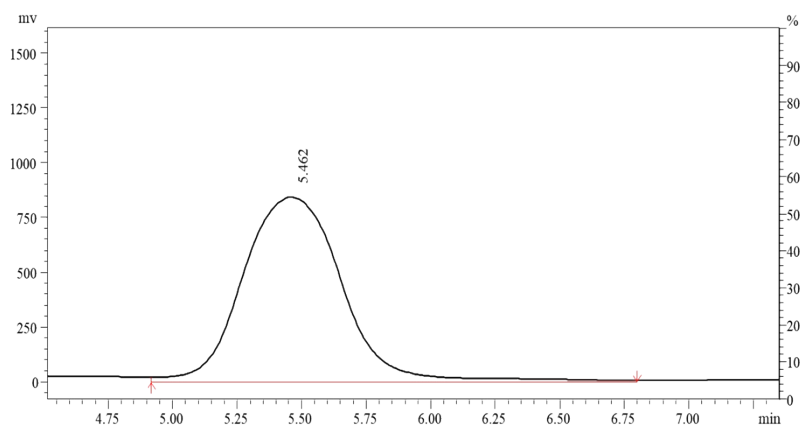


Figure S17 HPLC of phenyl methyl sulfoxide obtained over **ATGC-3** under UV irradiation (ee value >99%).

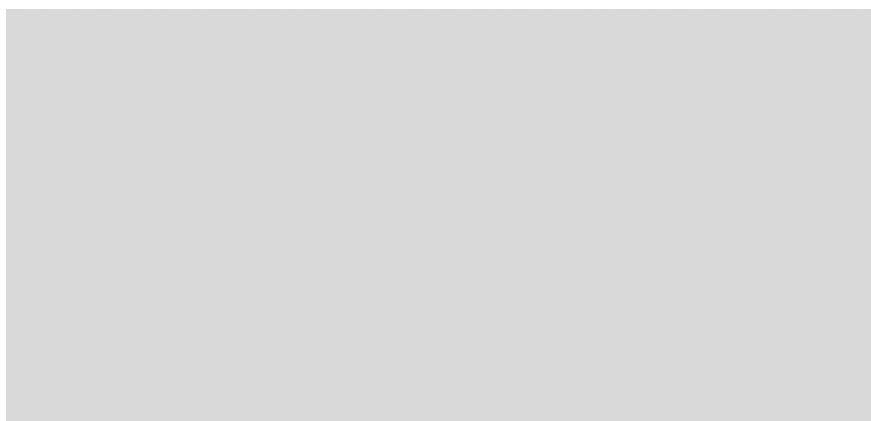


Figure S18 HPLC of phenyl methyl sulfoxide obtained over **ATGC-3** in dark (ee value = 78%).

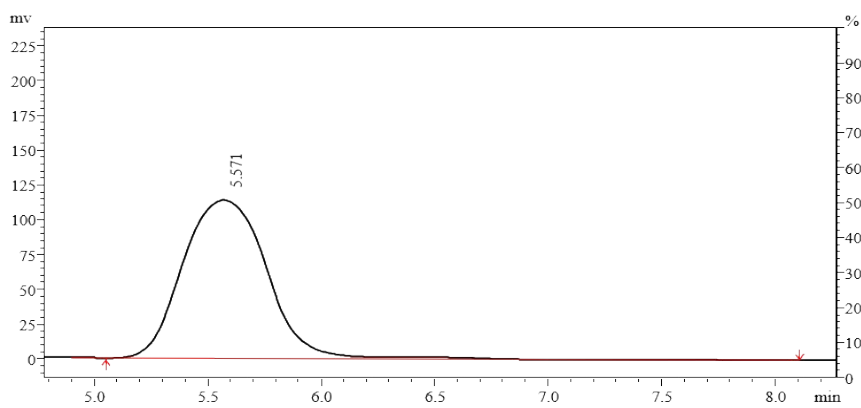


Figure S19 HPLC of phenyl methyl sulfoxide obtained over **ATGC-4** under UV irradiation (ee value > 99%).

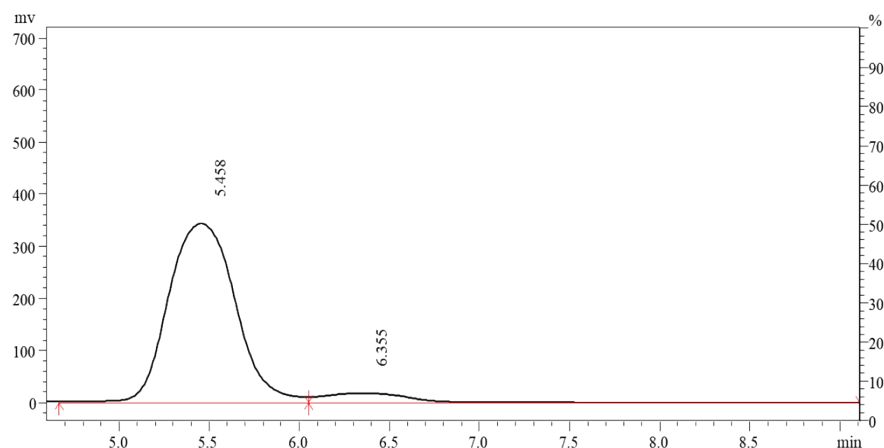


Figure S20 HPLC of phenyl methyl sulfoxide obtained over **ATGC-4** in dark (ee value =88%).

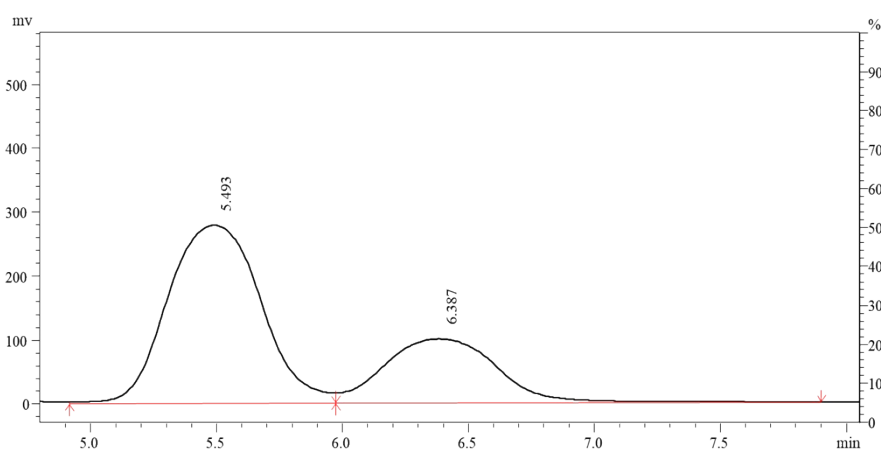


Figure S21 HPLC of phenyl methyl sulfoxide obtained over Neat-C in dark (ee value =39%).

Phenyl ethyl sulfoxide: The product has been identified by ^1H NMR spectrum (see Figure S22). ^1H NMR (CDCl_3 , 500 MHz): δ (ppm): 7.58-7.49 (m, 5 H, ArH), 2.88-2.76 (m, 2 H, $-\text{CH}_2-\text{CH}_3$), 1.18 (m, 3 H, $-\text{CH}_2-\text{CH}_3$). Chemoselectivity was determined by GC, nitrogen was used as the carrier gas with a flow of $30 \text{ mL} \cdot \text{min}^{-1}$, injector temperature and detector temperature were $250 \text{ }^\circ\text{C}$, column temperature was $150 \text{ }^\circ\text{C}$, $t_{\text{Phenyl ethyl sulfoxide}} = 6.6 \text{ min}$; ee value was determined by HPLC (*i*PrOH/ *n*-hexane = 1: 9 (v/v)); flow rate = $1.2 \text{ mL} \cdot \text{min}^{-1}$; $25 \text{ }^\circ\text{C}$; $\lambda = 254 \text{ nm}$; major enantiomer $t_R = 10.3 \text{ min}$

and minor enantiomer $t_S = 12.4$ min (see Figure S23-S25). $[\alpha]_D = +178.3$ ($c = 1.4$ in EtOH); lit: $[\alpha]_D = -169.1$ ($c = 1.4$ in EtOH) for (*S*), 82% ee.⁵

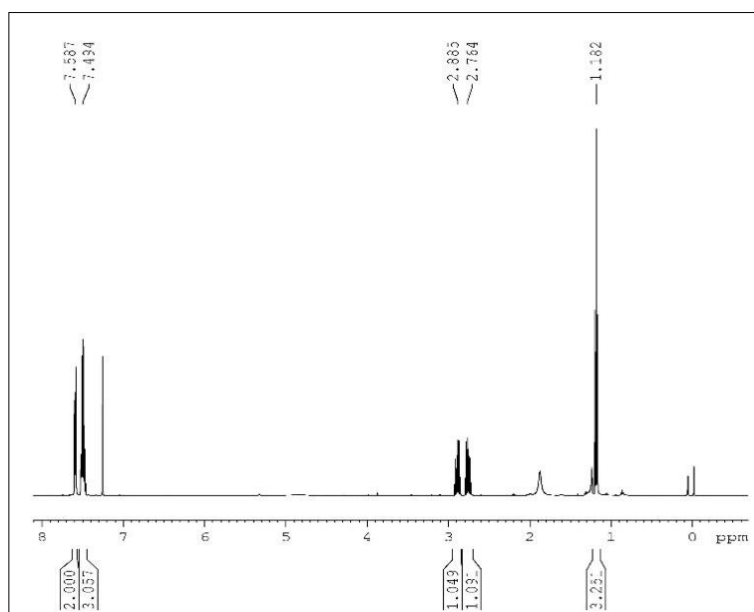


Figure S22 ¹H NMR of phenyl ethyl sulfoxide.

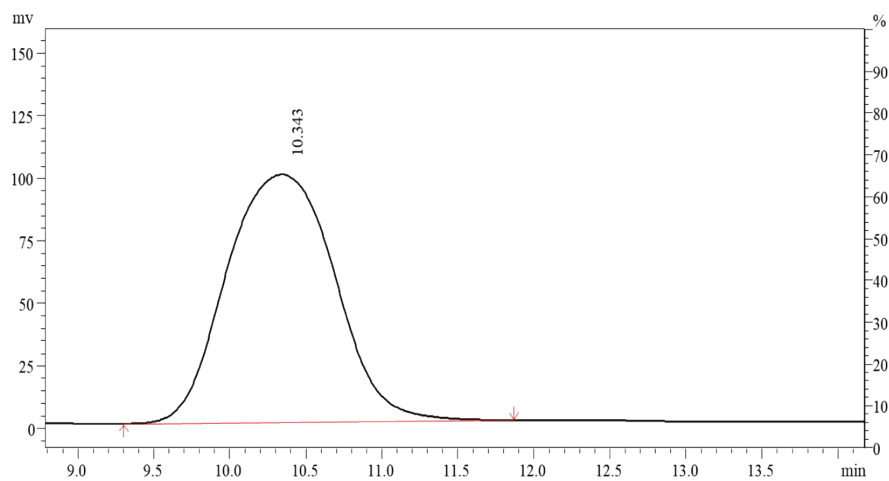


Figure S23 HPLC of phenyl ethyl sulfoxide obtained over ATGC-3 under UV irradiation (ee value >99%).

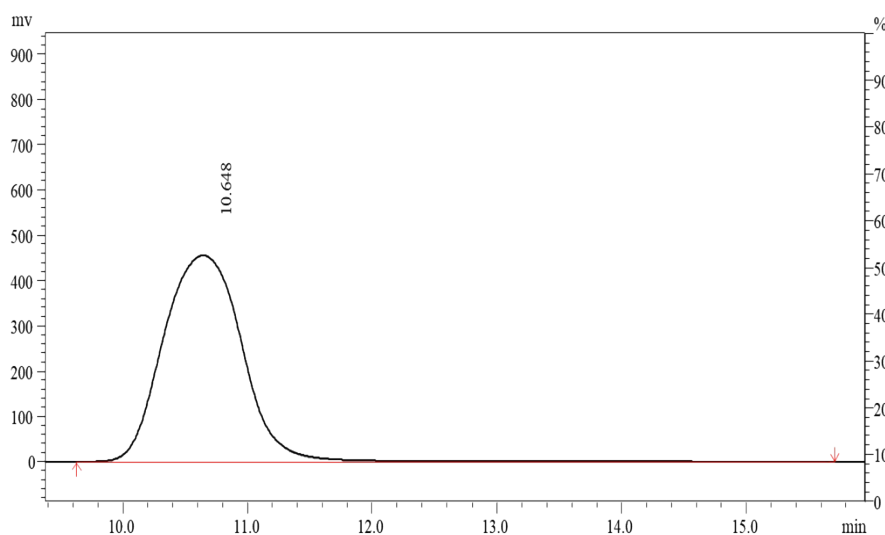


Figure S24 HPLC of phenyl ethyl sulfoxide obtained over **ATGC-3** in dark (ee value > 99%).

Phenyl n-butyl sulfoxide: The product has been identified by ^1H NMR spectrum (see Figure S25).

^1H NMR (CDCl_3 , 500 MHz): δ (ppm): 7.35-7.17 (m, 5 H, ArH), 2.96-2.93 (m, 2 H, $\text{CH}_3\text{-CH}_2\text{-CH}_2\text{-CH}_2\text{-S-}$), 1.68-1.64 (m, 2 H, $\text{CH}_3\text{-CH}_2\text{-CH}_2\text{-CH}_2\text{-S-}$), 1.49-1.46 (m, 2 H, $\text{CH}_3\text{-CH}_2\text{-CH}_2\text{-CH}_2\text{-S-}$), 0.96-0.93 (m, 3 H, $\text{CH}_3\text{-CH}_2\text{-CH}_2\text{-CH}_2\text{-S-}$). Chemoselectivity was determined by GC, nitrogen was used as the carrier gas with a flow of $30 \text{ mL} \cdot \text{min}^{-1}$, injector temperature and detector temperature were $250 \text{ }^\circ\text{C}$, column temperature was $180 \text{ }^\circ\text{C}$, $t_{\text{Phenyl } n\text{-butyl sulfoxide}} = 3.2 \text{ min}$; ee value was determined by HPLC (*i*PrOH/ *n*-hexane = 1: 9 (v/v)); flow rate = $1.2 \text{ mL} \cdot \text{min}^{-1}$; $25 \text{ }^\circ\text{C}$; $\lambda = 254 \text{ nm}$; major enantiomer $t_R = 5.44 \text{ min}$ and minor enantiomer $t_S = 5.93 \text{ min}$ (see Figure S26 and S27). $[\alpha]_D = +69.2$ (c = 1.8 in ethanol); lit: $[\alpha]_D = +64.4$ (c = 2.0 in ethanol) for (*R*), 90% ee.⁶

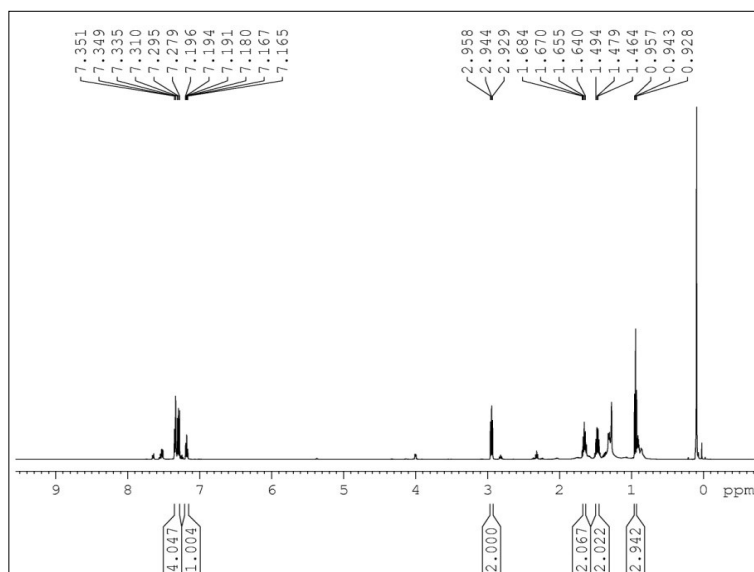


Figure S25 ^1H NMR of phenyl *n*-butyl sulfoxide.

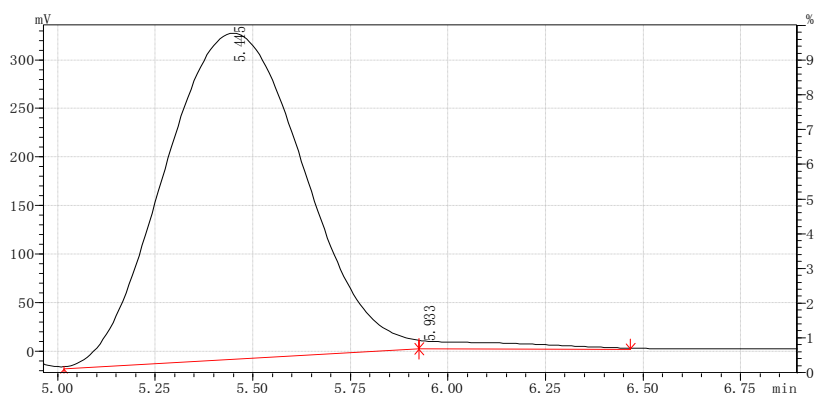


Figure S26 HPLC of phenyl *n*-butyl sulfoxide obtained over **ATGC-3** under UV irradiation (ee value = 97%).

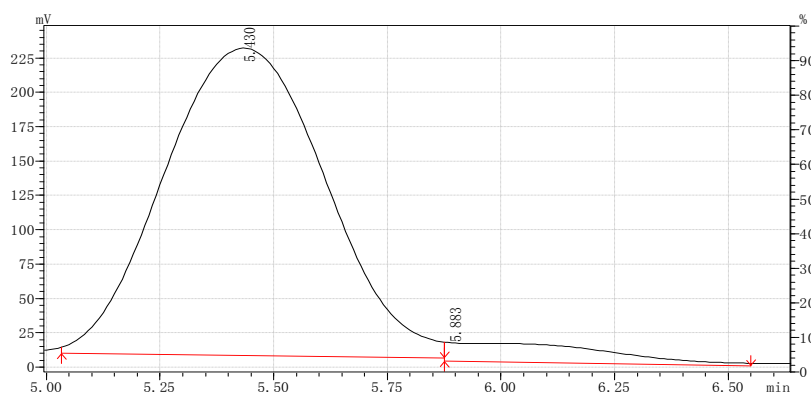


Figure S27 HPLC of phenyl *n*-butyl sulfoxide obtained over **ATGC-3** in dark (ee value = 85%).

Phenyl n-hexyl sulfide: The product has been identified by ^1H NMR spectrum (see Figure S28). ^1H NMR (CDCl_3 , 500 MHz): δ (ppm): 7.36-7.18 (m, 5 H, ArH), 2.97-2.94 (m, 2 H, $-\text{CH}_2-\text{CH}_2-\text{CH}_2-\text{S}-$), 1.71-1.64 (m, 2 H, $-\text{CH}_2-\text{CH}_2-\text{CH}_2-\text{S}-$), 1.49-1.43 (m, 2 H, $-\text{CH}_2-\text{CH}_2-\text{CH}_2-\text{S}-$), 1.37-1.35 (m, 4 H, $\text{CH}_3-\text{CH}_2-\text{CH}_2-$), 1.33-1.32 (m, 3 H, $\text{CH}_3-\text{CH}_2-\text{CH}_2-$). Chemoselectivity was determined by GC, nitrogen was used as the carrier gas with a flow of $30 \text{ mL} \cdot \text{min}^{-1}$, injector temperature and detector temperature were $250 \text{ }^\circ\text{C}$, column temperature was $180 \text{ }^\circ\text{C}$, $t_{\text{Phenyl } n\text{-hexyl sulfide}} = 4.5 \text{ min}$; ee value was determined by HPLC (*i*PrOH/ *n*-hexane = 1: 9 (v/v)); flow rate = $1.2 \text{ mL} \cdot \text{min}^{-1}$; $25 \text{ }^\circ\text{C}$; $\lambda = 254 \text{ nm}$; major enantiomer $t_R = 5.23 \text{ min}$ and minor enantiomer $t_S = 6.12 \text{ min}$ (see Figure S29 and S30). $[\alpha]_D = +98.3$ (c = 1.8 in ethanol).

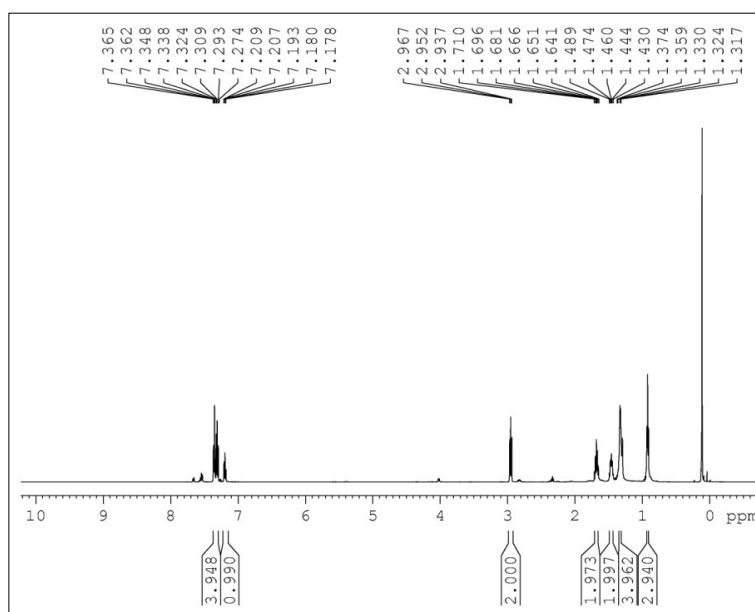


Figure S28 ^1H NMR of phenyl *n*-hexyl sulfoxide.

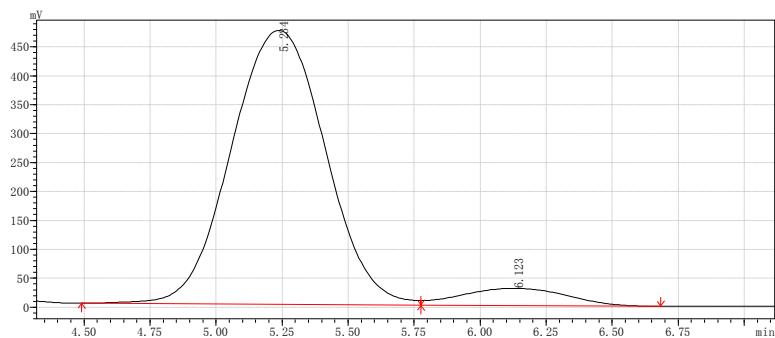


Figure S29 HPLC of phenyl *n*-hexyl sulfoxide obtained over **ATGC-3** under UV irradiation (ee value = 94%).

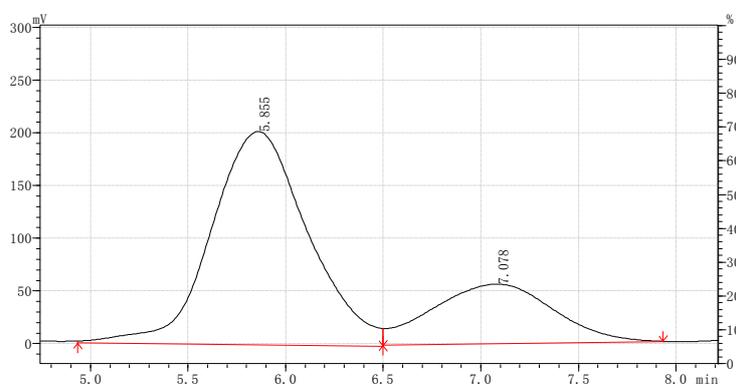


Figure S30 HPLC of phenyl *n*-hexyl sulfoxide obtained over **ATGC-3** in dark (ee value = 83%).

o-Methoxyphenyl methyl sulfoxide: The product has been identified by ^1H NMR spectrum (see Figure S31). ^1H NMR (CDCl_3 , 500 MHz): δ (ppm): 7.81-6.94 (m, 4 H, ArH), 3.89 (s, 3 H, $-\text{OCH}_3$), 2.78 (s, 3 H, $-\text{SCH}_3$). Chemoselectivity was determined by GC, nitrogen was used as the carrier gas with a flow of $30 \text{ mL}\cdot\text{min}^{-1}$, injector temperature and detector temperature were $250 \text{ }^\circ\text{C}$, column temperature was $150 \text{ }^\circ\text{C}$, $t_{o\text{-methoxyphenyl methyl sulfoxide}} = 8.1 \text{ min}$; ee value was determined by HPLC ($^i\text{PrOH}/ n\text{-hexane} = 2: 8 \text{ (v/v)}$); flow rate = $1.2 \text{ mL}\cdot\text{min}^{-1}$; $25 \text{ }^\circ\text{C}$; $\lambda = 254 \text{ nm}$; major enantiomer $t_R = 5.9 \text{ min}$ and minor enantiomer $t_S = 7.0 \text{ min}$ (see Figure S32 and S33). $[\alpha]_D^{25} = +321.3$ ($c=1.0$ in acetone); lit: $[\alpha]_D^{25} = +318.6$ ($c=1.0$ in acetone) for (*R*), 98% ee.⁷

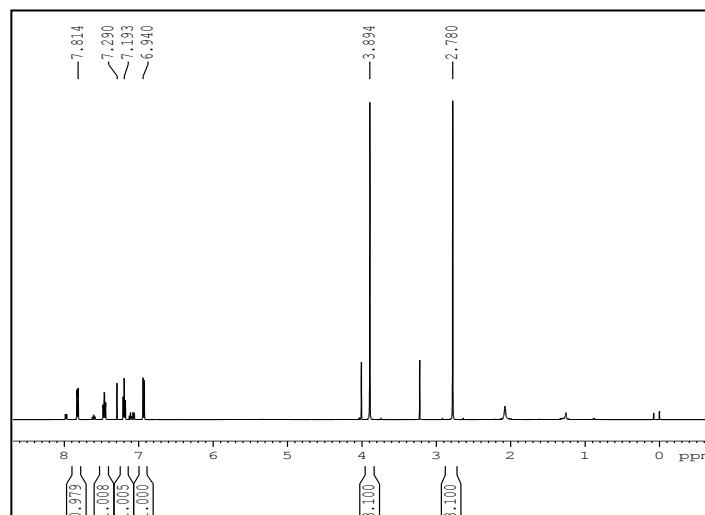


Figure S31 ^1H NMR of *o*-methoxyphenyl methyl sulfoxide.

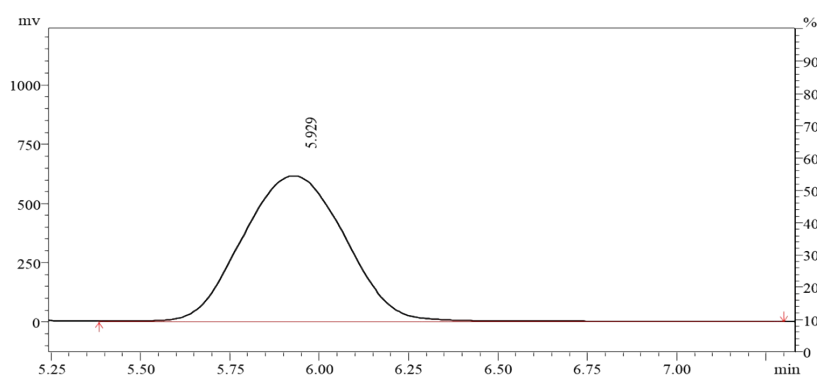


Figure S32 HPLC of *o*-methoxyphenyl methyl sulfoxide obtained over **ATGC-3** under UV irradiation (ee value > 99%).

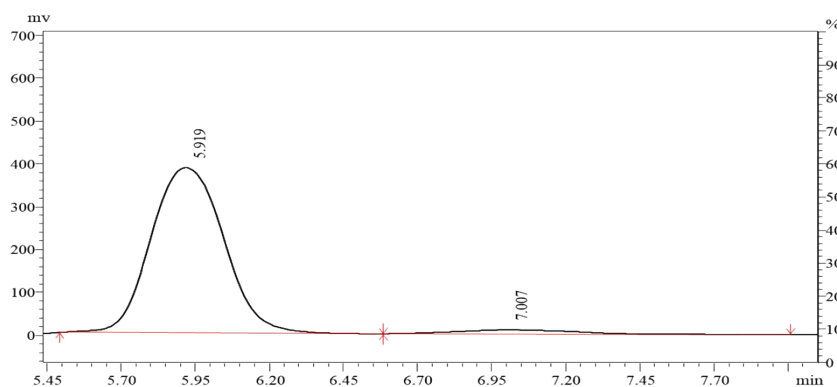


Figure S33 HPLC of *o*-methoxyphenyl methyl sulfoxide obtained over **ATGC-3** in dark (ee value = 93%).

p-Methoxyphenyl methyl sulfoxide: The product has been identified by ^1H NMR spectrum (see Figure S34). ^1H NMR (CDCl_3 , 500 MHz): δ (ppm): 7.88-7.06 (m, 4 H, ArH), 3.91 (s, 3 H, $-\text{OCH}_3$), 3.05 (s, 3 H, $-\text{SCH}_3$). Chemoselectivity was determined by GC, nitrogen was used as the carrier gas with a flow of $30 \text{ mL} \cdot \text{min}^{-1}$, injector temperature and detector temperature were $250 \text{ }^\circ\text{C}$, column temperature was $150 \text{ }^\circ\text{C}$, $t_{p\text{-methoxyphenyl methyl sulfoxide}} = 6.01 \text{ min}$; ee value was determined by HPLC ($^i\text{PrOH}/n\text{-hexane} = 2:8 \text{ (v/v)}$); flow rate = $1.2 \text{ mL} \cdot \text{min}^{-1}$; $25 \text{ }^\circ\text{C}$; $\lambda = 254 \text{ nm}$; major enantiomer $t_R = 6.8 \text{ min}$ and minor enantiomer $t_S = 7.9 \text{ min}$ (see Figure S35 and S36). $[\alpha]_D = +141.2$ ($c = 2.0$ in CHCl_3); lit: $[\alpha]_D = -129.7$ ($c = 2.0$ in CHCl_3) for (*S*), 86% ee.⁵

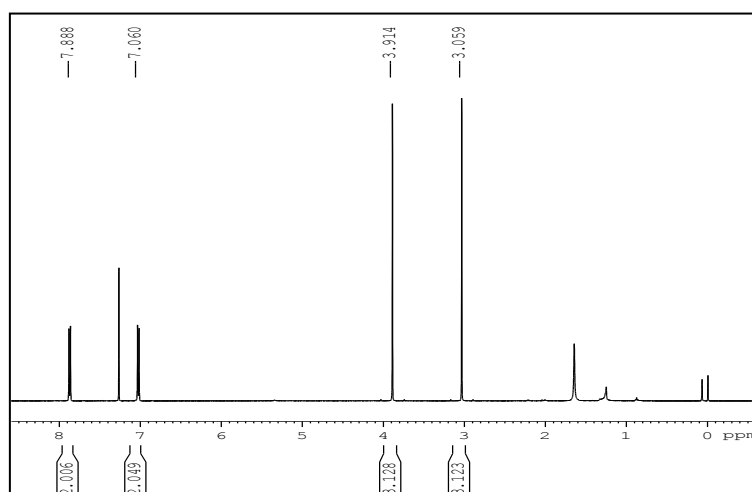


Figure S34 ^1H NMR of *p*-methoxyphenyl methyl sulfoxide.

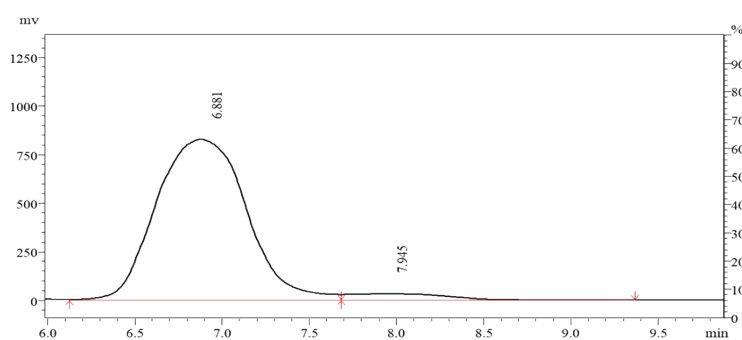


Figure S35 HPLC of *p*-methoxyphenyl methyl sulfoxide obtained over **ATGC-3** under UV

irradiation (ee value = 92%).

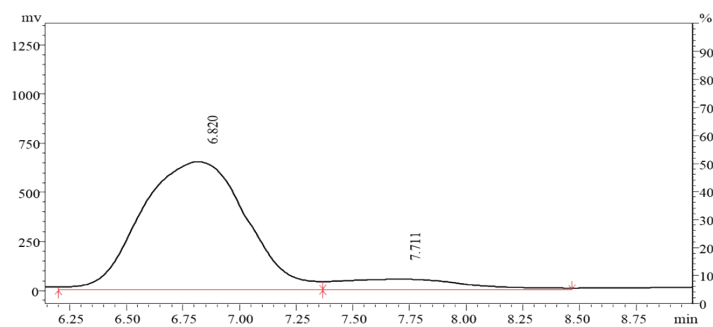


Figure S36 HPLC of methyl *p*-methoxyphenyl sulfoxide obtained over **ATGC-3** in dark (ee value = 82%).

p-Bromophenyl methyl sulfoxide: The product has been identified by ^1H NMR spectrum (see Figure S37). ^1H NMR (CDCl_3 , 500 MHz): δ (ppm): 7.65-7.52 (m, 4 H, ArH), 2.70 (s, 3 H, $-\text{SCH}_3$). Chemoselectivity was determined by GC, nitrogen was used as the carrier gas with a flow of 30 $\text{mL}\cdot\text{min}^{-1}$, injector temperature and detector temperature were 250 $^\circ\text{C}$, column temperature was 150 $^\circ\text{C}$, $t_{p\text{-bromophenyl methyl sulfoxide}} = 12$ min; ee value was determined by HPLC (*i*PrOH/ *n*-hexane = 1: 9 (v/v)); flow rate = 1.2 $\text{mL}\cdot\text{min}^{-1}$; 25 $^\circ\text{C}$; $\lambda = 254$ nm; major enantiomer $t_R = 12.2$ min and minor enantiomer $t_S = 16.0$ min (see Figure S38 and S39). $[\alpha]_D = +103.2$ (c = 1.0 in acetone); lit: $[\alpha]_D = -97.5$ (c = 1.8 in acetone) for (*S*), 94% ee.⁵

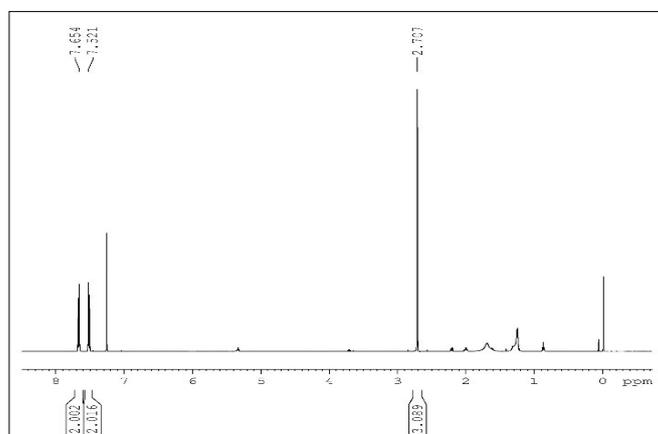


Figure S37 ^1H NMR of *p*-bromophenyl methyl sulfoxide.

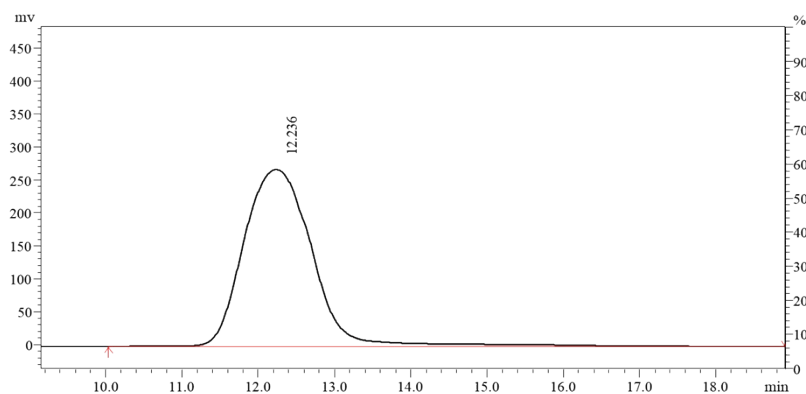


Figure S38 HPLC of *p*-bromophenyl methyl sulfoxide obtained over **ATGC-3** under UV irradiation (ee value >99%).

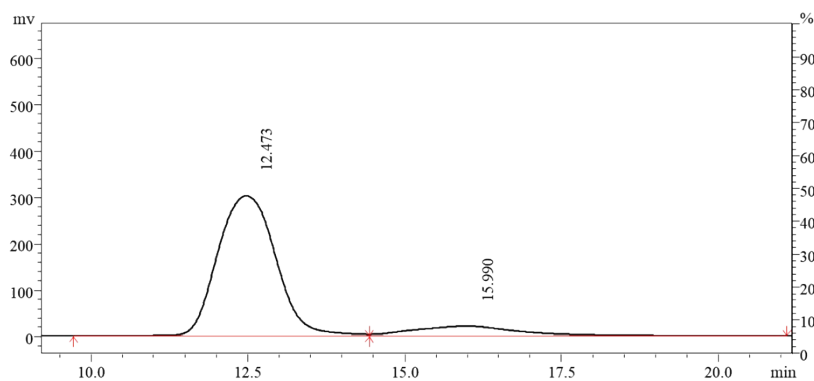
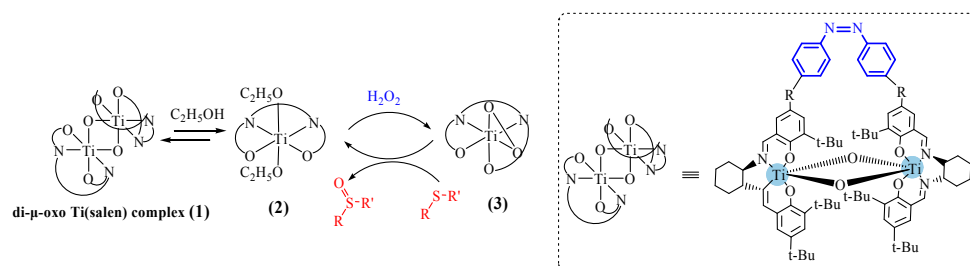


Figure S39 HPLC of *p*-bromophenyl methyl sulfoxide obtained over **ATGC-3** in dark (ee value =77%).

3.2 Proposed mechanism for the **ATGC-n**-catalyzed asymmetric sulfoxidation with H₂O₂ in ethanol upon UV irradiation

The UV-enforced synergistic effect of **ATGC-n** accorded with our hypothesis that the asymmetric sulfoxidation proceed through a bimetallic, cooperative mechanism, where di- μ -*oxo* Ti(salen) complex of [Ti(μ -O)₂(salen)₂] **1** was the real active catalyst for the transformation. As shown in Scheme S3, upon UV irradiation, the azobenzene linker was in *cis*-state. It located the two Ti(salen) units in proximity to each other, which was favorable for the formation of di- μ -*oxo*

Ti(salen) complex **1**. In the methanolic solution, di- μ -*oxo* Ti(salen) complex **1** was rapidly transformed to a monomeric Ti(salen) species **2** through rapid alkoxide exchange. Hydrogen peroxide was then reacted with the monomeric species **2**, giving the corresponding peroxy species **3** to oxidize the sulfides. Monomeric Ti(salen) species **2** was thus recovered, and it was readily changeable to the di- μ -*oxo* Ti(salen) complex **1** for catalyst recycle. Similar report has been made by B. Saito and co-worker.⁸



Scheme S3 Proposed mechanism for di- μ -*oxo* Ti(salen) complex mediated asymmetric sulfoxidation with H_2O_2 in ethanol.

3.3 Kinetic studies

Kinetic studies were used to further investigate the light-controlled cooperative catalysis over **ATGC-n**. The **ATGC-3** with different loadings (0.05, 0.07, 0.1 and 0.15 mol% of substrate) was stirred with phenyl methyl sulfide (1.0 mmol) in ethanol (2.0 mL) at 25 °C with/without UV irradiation. H_2O_2 (30 wt%, 1.2 mmol) was added at one time. Conversion of phenyl methyl sulfide was determined by GC. The values for the initial reaction rates at different catalyst loading were derived from the conversion plots (Table S1 and S2). Initial rate plots for the asymmetric oxidation of phenyl methyl sulfide catalyzed by **ATGC-3** with or without UV treatment were shown in Fig. S40.

The rate equation was considered as the sum of first- (intramolecular) and second- order (intermolecular) contributions and as a function of the total concentration of titanium ($[Ti]$):⁹⁻¹¹ rate = $k_{intra}[Ti] + k_{inter}[Ti]^2$. When the initial reaction rate is measured at different titanium concentrations $[Ti]$, plots of the rate/ $[Ti]$ versus $[Ti]$ should give linear correlations in which the y intercept is equal to the intramolecular rate coefficient (k_{intra}) and the slope corresponds to the intermolecular rate constant (k_{inter}).⁹⁻¹¹ Contribution of intra- and intermolecular reactions can be thus assessed quantitatively. As expected, for **ATGC-3** either UV-treated or in dark, the plots revealed linear correlations with positive slopes and non-zero y-intercepts (Fig. S40), which suggested the participation of both inter- and intramolecular pathways in sulfoxidation.^{10,11} Notably, the UV-treated **ATGC-3** displayed a larger intramolecular rate component ($k_{intra}=8.67 \text{ min}^{-1}$) than **ATGC-3** in dark ($k_{intra}=2.46 \text{ min}^{-1}$), consistent with UV-enforced intramolecular cooperative mode. While intermolecular reaction rate (k_{inter} , slope of plots) was decreased slightly when **ATGC-3** was treated with UV light, probably due to the steric hindrance of *cis*-**ATGC-3**, which reduced the stacking of neighbouring **ATGC-3** for intermolecular cooperative function.¹²

Table S1 Kinetics measurement of **ATGC-3** in asymmetric oxidation of phenyl methyl sulfide with H_2O_2 in ethanol under UV irradiation ^a

Catalyst loading ^b [M]	Reaction time (min)	Conversion ^c (%)	Initial rate constants (K_{obs})	$K_{obs}/[M]$
0.05	10	16	1.46	11.73
	20	30		
	30	42		
	40	55		
	50	65		
	60	70		
0.07	10	24	2.43	13.90
	20	42		
	30	58		
	40	70		

	50	78		
	60	83		
0.1	10	37	4.18	16.74
	20	58		
	30	75		
	40	84		
	50	91		
	60	98		
0.15	10	58	7.23	19.29
	20	76		
	30	89		
	40	97		
	50	99		
	60	100		

^a phenyl methyl sulfide (1.0 mmol), H₂O₂ (30 wt%, 1.2 mmol, added at one portion), ethanol (2.0 mL), 60 min, 25 °C, UV irradiation. ^b 0.05, 0.07, 0.10, or 0.15 mol% of substrate, based on titanium content. ^c Determined by GC.

Table S2 Kinetics measurement of **ATGC-3** in asymmetric oxidation of phenyl methyl sulfide with H₂O₂ in ethanol in dark ^a

Catalyst loading ^b [M]	Reaction time (min)	Conversion ^c (%)	Initial rate constants ^d (<i>K</i> _{obs})	<i>K</i> _{obs} /[M]
0.05	10	9	1.00	8.03
	20	16		
	30	22		
	40	26		
	50	29		
	60	32		
0.07	10	18	2.07	11.85
	20	29		
	30	35		
	40	39		
	50	44		
	60	47		
0.1	10	30	3.78	15.13
	20	46		
	30	55		
	40	60		

	50	63		
	60	68		
	10	55		
	20	68		
0.15	30	74	7.92	21.123
	40	75		
	50	78		
	60	80		

^a Phenyl methyl sulfide (1.0 mmol), H₂O₂ (30 wt%, 1.2 mmol, added at one portion), ethanol (2.0 mL), 60 min, 25 °C, in dark. ^b 0.05, 0.07, 0.10, or 0.15 mol% of substrate, based on titanium content. ^c Determined by GC. ^d The initial rate constants (K_{obs}) were obtained by calculation of the tangent in $t=0$ for the conversion plots obtained by GC.

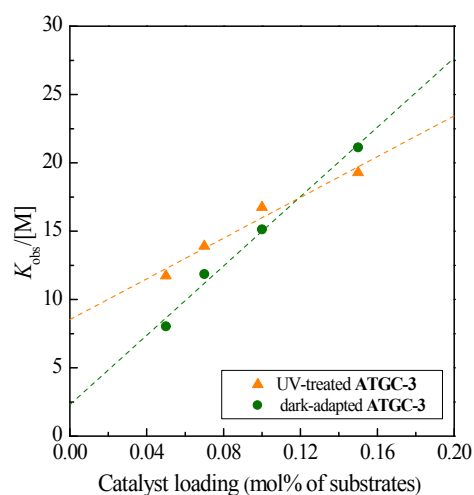


Fig. S40 Initial rate plots for the asymmetric oxidation of phenyl methyl sulfide catalyzed by **ATGC-3** with or without UV treatment.

3.4 Computational Studies

Density functional theory (DFT) was employed to optimize the structures of bimetallic **ATGC-n** ($n=0, 2, 3,$ and 4). The simulated structures were performed with B3LYP hybrid functional, where Ti, O, and N used 6-31 g* basis set, C used 3-21 g* basis set. For all DFT calculations, a convergence

criterion of 1.0×10^{-6} a.u. was adopted for changes in energy and density matrix elements. The optimized three-dimensional structure modes of the bimetallic catalysts were showed in Figure S41, and the corresponding $\text{Ti}^{\text{IV}}\text{-Ti}^{\text{IV}}$ distance were listed in Table S3. Indeed, *cis*-azobenzene linker located two $\text{Ti}(\text{salen})$ units in proximity to each other. Two metallosalen units in *cis*-**ATGC-3** were aligned face to face in a head-to-tail orientation with a minimum $\text{Ti}^{\text{IV}}\text{-Ti}^{\text{IV}}$ distance of 6.42 Å, as shown by the optimized, computed structure (Table S3). Such a spatial arrangement of two active centers was obviously favourable for cooperative function and thereby enforced a subsequent intramolecular, cooperative reaction pathway to realize high catalytic activity and selectivity. Further increasing the spacer length of **ATGC-n** ($n=4$) was detrimental to the intramolecular bimetallic cooperation due to the long metal-metal distance (6.48 Å). Furthermore, the enlarged linker allowed for back-folding to give the “head-to-head” orientation, which might be also unfavourable for the cooperative effect.

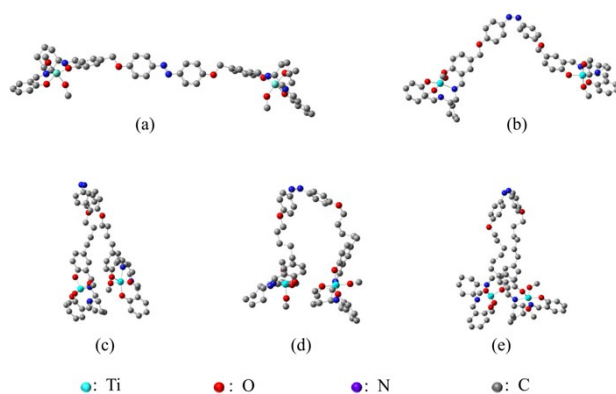


Figure S41 The optimized molecular structure of the *trans*-**ATGC-0** (a), *cis*-**ATGC-0** (b), *cis*-**ATGC-2** (c), *cis*-**ATGC-3** (d), and *cis*-**ATGC-4** (e)

Table S3 $\text{Ti}^{\text{IV}}\text{-Ti}^{\text{IV}}$ distance of the **ATGC-n** ($n=0, 2, 3,$ and 4) modes

Modes	<i>trans</i> - ATGC-0	<i>cis</i> - ATGC-	<i>cis</i> - ATGC-2	<i>cis</i> - ATGC-3	<i>cis</i> - ATGC-4
-------	------------------------------	---------------------------	----------------------------	----------------------------	----------------------------

0					
Ti ^{IV} -Ti ^{IV} distance (Å)	26.9	19.6	7.05	6.42	6.48

References

- (1) Y. Zhang, R. Tan, M. Gao, P. Hao and D. Yin, *Green Chem.*, 2017, **19**, 1182.
- (2) C. Lv, D. Xu, S. Wang, C. Miao and C. Xia, *Catal. Commun.*, 2011, **12**, 1242-1245.
- (3) S. Colonna and R. Fornasier. *Synthesis*, **1975**, 8, 531-532.
- (4) S. Seiji, N. Shinchiro, N. Mikio and M. Osamu, *Bull. Chem. Soc. Jpn.*, 1985, **58**, 2340-2347.
- (5) J. Legros and C. Bolm, *Chem. Eur. J.*, 2005, **11**, 1086-1092.
- (6) T. Sugimoto, T. Kokubo, J. Miyazaki, S. Tanimoto and M. Okano, *J. Chem. Soc., Chem. Commun.*, 1979, 402-404.
- (7) J. M. Brunel and H. B. Kagan, *Bull. Soc. Chim. Fr.*, 1996, **133**, 1109-1115.
- (8) B. Saito and T. Katsuki, *Tetrahedron Lett.*, 2001, **42**, 8333-8336.
- (9) R. M. Haak, S. J. Wezenberg and A. W. Kleij, *Chem. Commun.*, 2010, **46**, 2713;
- (10) S. J. Wezenberga and A. W. Kleij, *Adv. Synth. Catal.*, 2010, **352**, 85;
- (11) J. Burés, *Angew. Chem. Int. Ed.*, 2016, **55**, 2028.
- (12) L. Lin, Z. Yan, J. Gu, Y. Zhang, Z. Feng and Y. Yu, *Macromol. Rapid Commun.*, 2009, **30**, 1089.